Palaeontology
The Palaeontological Association
www.palass.org
[Palaeontology, Vol. 68, Part 1, 2025, e12734]

# Accelerations of the Phanerozoic biogeosystems

*by* HAITAO SHANG*

Department of Earth, Environmental and Resource Sciences, and Computational Science Program, The University of Texas at El Paso, El Paso, TX 79968, USA; htshang.research@gmail.com

Typescript received 11 March 2024; accepted in revised form 21 October 2024

**Abstract:** Biogeosystems underwent significant changes during the Phanerozoic Eon. Substantial efforts have been dedicated to reconstructing the biological metrics and environmental variables characterizing the evolutionary trajectories of deep-time biogeosystems and investigating the mechanisms responsible for variations in these quantities. The accelerations (i.e. rates of change in the variation rates) of these quantities, however, have rarely been studied. This work explores the dynamical modes and statistical properties of the accelerations of genus richness, origination, extinction, atmospheric $CO_2$ level, and global average temperature in the Phanerozoic. Statistical assessments show that the accelerations of these quantities systematically exhibit scale-invariant behaviours. Moreover, correlation analyses indicate that the accelerations of genus richness, origination, extinction, and global average temperature are moderately or weakly correlated with one another, while they are all uncorrelated with the acceleration of the atmospheric $CO_2$ level. These results suggest that the acceleration is an effective concept for probing biological and geological evolution and offers insights into the internal interactions, dynamics, and stability of the Phanerozoic biogeosystems.

**Key words:** acceleration, Phanerozoic Eon, biogeosystem, scale invariance, temporal correlation.

THE Phanerozoic represents a unique chapter in Earth's history; biogeosystems experienced dramatic variations during this eon. Considerable efforts have been devoted to understanding the long-term patterns of the Phanerozoic marine animals' genus richness, origination intensity, and extinction intensity (Simpson 1944; Foote 2000; Sepkoski 2002; Alroy *et al.* 2008; Fan *et al.* 2020). With the reconstructed time series of these biological metrics, studies have revealed many intriguing macroevolutionary patterns of Phanerozoic life such as contingency (Vermeij 2006; Blount *et al.* 2018), periodicity (Raup & Sepkoski 1984; Rohde & Muller 2005), quantum evolution (Simpson 1944, 1953; Fitch & Ayala 1995), and punctuated equilibrium (Gould & Eldredge 1977; Gould 2002; Duran-Nebreda *et al.* 2024). Significant events in life evolution are often accompanied by remarkable variations in the environment (Bambach 2006; Benson *et al.* 2021). Modern geochemical techniques and mathematical models are extraordinarily successful at inferring the evolutionary trajectories of environmental variables such as the atmospheric $CO_2$ level and global average temperature. Studies have suggested that these two environmental variables and the three biological metrics (i.e. genus richness, origination intensity, and extinction intensity) are tightly interlocked and therefore their variations are temporally correlated over geologic time (Bambach 2006; Hannisdal & Peters 2011; Bond & Grasby 2017). For instance, a natural ecosystem hosting more diverse species stores a larger amount of carbon and therefore lowers the $CO_2$ level (Cardinale *et al.* 2012; Hooper *et al.* 2012), influencing the biogeochemical cycles of carbon and other elements coupled with it. The other example is that a significant increase in temperature may result in mass extinctions (Penn *et al.* 2018; Song *et al.* 2021) due to the limited metabolic and physiological tolerances of life to high temperature (Sheridan & Bickford 2011; Deutsch *et al.* 2015).

Studies of deep-time biogeosystems usually focus on the reconstruction and analyses of evolutionary trajectories of biological metrics and environmental variables. Time series of these quantities and their variations or variation rates have been used to distill information about the stability, dynamics, and interactions of different components of the global Earth-life system (Payne *et al.* 2020; Mills *et al.* 2021; Shang 2024a). Less attention, however, has been paid to the rates of change in variation rates, which is defined as *accelerations* in this study (see Datasets, below). Here, I analyse the accelerations of genus richness, origination, extinction, atmospheric $CO_2$ level, and global average temperature during the Phanerozoic, investigate the distributions and temporal correlation of these accelerations, and show that the accelerations of these five quantities offer a new window through which to explore the fundamental mechanisms regulating the evolution of deep-time biogeosystems.


doi: 10.1111/pala.12734

This work is organized as follows. Material & Method describes the procedures of data processing, distribution fitting, comparison and selection of the best-fitting distributions, goodness-of-fit tests, and analysis of temporal correlations among the accelerations. In Scale-Invariant Patterns, I show that the power law or exponentially truncated power law offers the best-fitting distribution for the accelerations of the five quantities according to the Bayesian information criterion (BIC) and likelihood-ratio test (LRT). In Temporal Correlations, I analyse the temporal correlations among the five quantities' accelerations and show that the accelerations of genus richness, origination, extinction, and global average temperature are moderately or weakly correlated to each other, but uncorrelated with the acceleration of the atmospheric $CO_2$ level. These statistical results suggest that the distributions of the three biological metrics are unlikely to connect to the distribution of the atmospheric $CO_2$ level but are probably influenced by the distribution of the global average temperature to some extent. Finally, I discuss the Implications of the patterns and relations of the five quantities' accelerations for the internal interactions, dynamics, and stability of the Phanerozoic biogeosystems.

## MATERIAL & METHOD

### *Datasets*

The original datasets on the biological metrics of the Phanerozoic marine animals are from the Paleobiology Database (https://paleobiodb.org). These datasets were standardized using the R package divDyn developed by Kocsis *et al.* (2019) to obtain the time series of biological metrics used in this study. The reconstructed datasets on atmospheric $CO_2$ level and global average temperature during the Phanerozoic are from the studies by Foster *et al.* (2017) and Scotese *et al.* (2021), respectively. The overall time range and time step size of each time series are summarized in Table S1. These time series do not span the entire Phanerozoic and their time steps are not the same. I used smoothing splines (with the identical time step), which have been shown to be effective for fitting these quantities (Rohde & Muller 2005; Foster & Rohling 2013; Vérard & Veizer 2019), to interpolate the original time series to obtain data at the same time points so that the patterns of these time series are comparable and their temporal correlations can be analysed. For the results presented in the main text, the time series are interpolated with a time step size of 0.1 million years (myr).

Selecting an appropriate time step size for the time series interpolation involves a trade-off in this study. A larger time step size, such as 1 myr, seems to be more proper than 0.1 myr for mimicking the stratigraphic resolution in reality. However, using such a large time step will reduce the number of data points in time series, which may cause problems when analysing the distribution of this small dataset. For example, the power law and exponentially truncated power law distributions (employed in this study and introduced under Candidate Distributions, below) usually span several orders of magnitude and therefore require appropriately large datasets so that the counts in the bins of histograms will be sufficiently large and can be properly fitted with these distributions. Thus, I used 0.1 myr rather than 1 myr as the time step size to interpolate the time series, and the results presented in the main text come from the analysis of the time series interpolated with 0.1 myr as the time step size. To test the sensitivity of the statistical results to the time step size, I interpolated the time series using two other time step sizes, 0.05 and 0.01 myr; the analysis of these time series with smaller time step sizes is reported in the Supporting Information. One should note that these time series fitted using smaller time step sizes are only for the purpose of evaluating the sensitivity of the results to the time step size; in practice, such high resolutions of the stratigraphic age are difficult to achieve.

I denote the time series of one quantity by $\{\psi_i\}$ and the difference between two consecutive data points in this time series by $\Delta\psi_i = \psi_{i+1} - \psi_i$. As discussed above, the time step size, which is denoted by $\Delta t = t_{i+1} - t_i$, equals 0.1, 0.05 or 0.01 myr. The variation rate at time $t_i$, which measures the variation in $\psi_i$ during the unit time $\Delta t$, is expressed as $\Delta R_i = \frac{\Delta\psi_i}{\Delta t}$. The acceleration, which represents the rate of change in $R_i$ during $\Delta t$, is then:

$$a_i = \frac{\Delta R_i}{\Delta t} = \frac{\Delta^2 \psi_i}{\Delta t^2}$$

Analogous to the concept of acceleration in Newtonian mechanics, the acceleration defined in the above equation characterizes how the variation rates of biological metrics and environmental variables change over geologic time. I classify $a_i$'s of each variable into three groups: negative acceleration (NA), positive acceleration (PA), and all acceleration (AA); the $a_i$'s that fall into these three categories are denoted by NA $= \{a_i | a_i < 0\}$, PA $= \{a_i | a_i > 0\}$, and AA $= \{a_i | a_i \neq 0\}$, respectively. The logarithm of a negative value is mathematically undefined; thus the absolute values of data in these three categories, which are denoted as |NA| $= \{|a_i| \mid a_i < 0\}$, |PA| $= \{a_i \mid a_i > 0\}$, and |AA| $= \{|a_i| \mid a_i \neq 0\}$, are used for analyses. The |AA| category is defined as a set that does not contain zero values (i.e. $a_i \neq 0$) because the logarithm of a zero is mathematically undefined. However, in this study, no zero values appear in the accelerations of all five quantities obtained from the time series interpolated

with the time step size of 0.1, 0.05 or 0.01 myr; therefore, no $a_i$ values are discarded here.

### *Candidate distributions*

To investigate the distributions of the five quantities' accelerations, I first grouped $|a_i|$'s in each category into ten bins with equal width (i.e. equally spaced along the acceleration axis in a histogram) and denoted the middle point of the $k$-th bin as $\alpha_k$ and the count (i.e. the number of data points) in this bin as $N_k$. The data points of $(\alpha_k, N_k)$ in each category of accelerations of the five quantities all appear as straight lines on log–log plots, suggesting that power-law patterns may exist in these accelerations. The power law distribution is a type of heavy-tailed distribution which is characterized by tails that are not exponentially bounded (Bryson 1974; Asmussen 2003). The exponential distribution is the minimum alternative for testing heavy-tailed distributions (Clauset *et al.* 2009; Alstott *et al.* 2014). If a power law distribution does not fit a given dataset better than an exponential distribution, then any heavy-tailed distribution is unlikely to be a good fit for this dataset (Clauset *et al.* 2009; Alstott *et al.* 2014). Moreover, although a straight line on a log–log plot is a key feature of power-law patterns, other heavy-tailed distributions, such as lognormal and stretched-exponential distributions, are able to produce datasets possessing distributions that are close to the power law (Bryson 1974; Asmussen 2003). Furthermore, the power law distribution sometimes does not span the whole range of a given dataset; instead, it exists over a certain interval and is truncated by an exponential bounded tail. This type of distribution, which is referred to as the exponentially truncated power law, implies the existence of underlying mechanisms or constraints preventing the occurrence of extremely large events (Sornette & Cont 1997; Deluca & Corral 2013). As mentioned above, this study shows that the accelerations of the three biological metrics and two environmental variables during the Phanerozoic exhibit the power law or exponentially truncated power law distributions. Therefore, the rest of this section focuses on these two distributions; further details about the lognormal, exponential, and stretched-exponential distributions are provided in Clauset *et al.* (2009) and Forbes *et al.* (2011).

Mathematically, the power law is expressed as $P(x) \sim x^{-\alpha}$, where $\alpha > 0$ is the exponent. On a log–log plot, the power law distribution is manifested by a straight line and can be written as $\log P(x) \sim -\alpha \log x$ , which is also referred to as the scale-invariant pattern and implies that the underlying mechanism regulating such a relation is independent of a specific scale (Clauset *et al.* 2009; Schroeder 2009). Power laws are ubiquitous in natural systems (Middelburg 1989; West 1999; Glazier 2005; Shang 2023a, 2024b). For example, the metabolic rate versus body mass of animals (West 1999; Glazier 2005) and the degradation rate versus age of organic matter in ecosystems (Middelburg 1989; Shang 2023a) exhibit power-law patterns. To interpret the principles responsible for power laws, several theories, such as self-organized criticality (Bak *et al.* 1987) and highly optimized tolerance (Carlson & Doyle 1999), have been proposed. Although these theories offer plausible explanations for the scale-invariant behaviours in some systems, the mechanisms responsible for many power-law patterns remain unclear.

Exponentially truncated power laws are typically written as $P(x) \sim \exp(-\lambda x) \times x^{-\alpha}$, where $\alpha > 0$ and $\lambda > 0$ are the exponent and cutoff parameter, respectively. In the exponentially truncated power law, the power-law behaviour appears only over a range where the $x$ values are relatively small; beyond a certain value of $x$, the distribution is limited by an exponentially decaying tail and falls off much faster than the power law distribution, reflecting the existence of some constraints (Newman 2005; Clauset *et al.* 2009). In other words, the exponentially truncated power law distribution exhibits the scale-invariant pattern only in a certain range where the exponential term $\exp(-\lambda x)$ does not effectively influence the behaviour of the power-law term $x^{-\alpha}$ (Newman 2005; Clauset *et al.* 2009). Exponentially truncated power laws exist in a variety of natural systems; for example, the sizes of wildfires and the intensities of solar flares have been shown to follow exponentially truncated power law distributions (Clauset *et al.* 2009).

### *Distribution comparison & selection*

To determine which of these five distributions (i.e. power law, exponentially truncated power law, exponential, stretched-exponential, or lognormal) best fits the accelerations of the three biological metrics and two environmental variables, I calculated the BIC and performed the LRT. The BIC is defined as $\mathrm{BIC} = -2 \ln\left(\widehat{\mathscr{L}}\right) + k \ln(n)$, where $\widehat{\mathscr{L}}$ is the likelihood of the model given the dataset, $k$ is the number of estimated parameters in the model, and $n$ is the number of data points (Schwarz 1978; Neath & Cavanaugh 2012). The BIC is a statistical metric balancing the fit and complexity of a specific mathematical model through incorporating the likelihood of this model for a given dataset and the number of parameters involved (Schwarz 1978; Neath & Cavanaugh 2012). To prevent overfitting, the BIC penalizes models possessing more parameters and prefers simpler models that can explain the data well (Schwarz 1978; Neath & Cavanaugh 2012). In this study, the distribution with the lowest BIC value is selected as the best model for a given dataset.

The LRT is a statistical method used to compare the goodness of fit of two models for a given dataset (Buse 1982; Lewis *et al.* 2011). Here, the LRT statistic for distribution A versus distribution B is expressed as $LRT\,(\mathrm{A},\mathrm{B}) = \log\left[\mathscr{L}_\mathrm{B}\left(\mathrm{D}|\widehat{\Psi_\mathrm{B}}\right)/\mathscr{L}_\mathrm{A}\left(\mathrm{D}|\widehat{\Psi_\mathrm{A}}\right)\right]$, in which D represents a given dataset; $\mathscr{L}_\mathrm{A}$ and $\mathscr{L}_\mathrm{B}$ are the likelihoods of distributions A and B, respectively, fitted using the maximum likelihood estimation; and $\widehat{\Psi_\mathrm{A}}$ and $\widehat{\Psi_\mathrm{B}}$ are the parameter values maximizing $\mathscr{L}_\mathrm{A}$ and $\mathscr{L}_\mathrm{B}$, respectively, in the parameter space. If $LRT < 0$, then distribution B fits dataset D better than distribution A; however, if $LRT > 0$, then distribution A outperforms distribution B for dataset D. Since the random variations in sample data can influence the $LRT(\mathrm{A},\mathrm{B})$ and its interpretations, the *LRT* needs to be standardized with the standard deviation (Vuong 1989; Clauset *et al.* 2009), which gives a p-value that indicates the statistical significance of the sign of $LRT\,(\mathrm{A},\mathrm{B})$. Following the convention, I set the significance level for the p-value to 0.05. If $p \geq 0.05$, then the sign of $LRT\,(\mathrm{A},\mathrm{B})$ is likely to result from chance fluctuations, suggesting that the test is inconclusive and both distributions A and B probably offer plausible fits for the given dataset. However, if $p < 0.05$, then the sign of $LRT\,(\mathrm{A},\mathrm{B})$ is unlikely to be caused by random variations, implying that the test is conclusive and one distribution outperforms the other for the given dataset. In this study, the LRTs are conducted using the Python package Powerlaw developed by Alstott *et al.* (2014).

### *Goodness-of-fit tests*

To evaluate the goodness of fit of the distributions, I calculated the coefficient of determination ($R^2$) and root mean square error (RMSE). The $R^2$ measures the fraction of variations in the dependent variable explained by a distribution, and the RMSE measures the distance between real and predicted values. A larger $R^2$ and a smaller RMSE indicate a better fit (Freund & Wilson 2003). Moreover, I performed the Kolmogorov–Smirnov (KS) test (Massey 1951) and Cramér–von Mises (CM) two-sample test (Anderson 1962) to assess whether a distribution adequately describes the datasets. The KS and CM statistics use different metrics to measure the distance between the cumulative distribution function (CDF) of the samples and the CDF of the distribution. I set the critical p-value for the KS and CM tests to 0.05 in this study. If $p \geq 0.05$, then I conclude the CDFs of the samples and the tested distribution are likely to be the same and thus the tested distribution adequately describes the data; however, if $p < 0.05$ , then I conclude that the CDFs of the samples and the tested distribution are unlikely to be the same and therefore the tested distribution poorly depicts the data.

### *Correlation analysis*

To investigate the temporal correlations among the quantities, I computed the Pearson correlation coefficient (i.e. Pearson's $r$) and Spearman's rank correlation coefficient (i.e. Spearman's $\rho$). The Pearson correlation analysis assumes that the variables either follow the standard normal distribution or are approximately normally distributed (Freedman 2009; McElreath 2018). However, the five quantities and their accelerations do not satisfy such an assumption. Therefore, the correlation analysis in this study is primarily based on the Spearman's rank correlation coefficient, which does not require the dataset to meet the normality assumption (Freedman 2009; McElreath 2018). The results from the Pearson correlation analysis are presented in the Supporting Information for reference. For the values of Pearson's $r$ and Spearman's $\rho$, $r = -1$ or $\rho = -1$ suggests a perfect negative correlation between two quantities, while $r = 1$ or $\rho = 1$ implies a perfect positive correlation between two quantities. Again, I set the critical p-value for these two tests to 0.05. If $p < 0.05$, then I conclude that a significant correlation exists; otherwise, I conclude that there is no significant correlation between two quantities.

## RESULTS & DISCUSSION

### *Scale-invariant patterns*

Figure 1 shows the time series of the absolute values of accelerations (defined in Datasets, above) for genus richness, origination, extinction, atmospheric $CO_2$ level, and global average temperature during the Phanerozoic Eon. The information about the original datasets of these five quantities is summarized in Table S1. The procedure for data processing is described above. In this section, I show that the accelerations of the three biological metrics and two environmental variables systematically exhibit power laws or exponentially truncated power laws. To avoid ambiguity, the power law distribution is henceforth referred to as the pure power law.

First, I classified the accelerations of each quantity into three categories: negative acceleration (|NA|), positive acceleration (|PA|), and all acceleration (|AA|). Their definitions are provided under Datasets, above. Figure 2 shows the patterns of the five quantities' accelerations on log–log plots. In each panel of Figure 2, the horizontal-axis and vertical-axis values for each data point are the midpoint and count, respectively, of each bin for the accelerations. The grey dashed lines and black dashed curves are the best-fitting pure and exponentially truncated power laws, respectively, for given data points. The mathematical expressions of these distributions and their

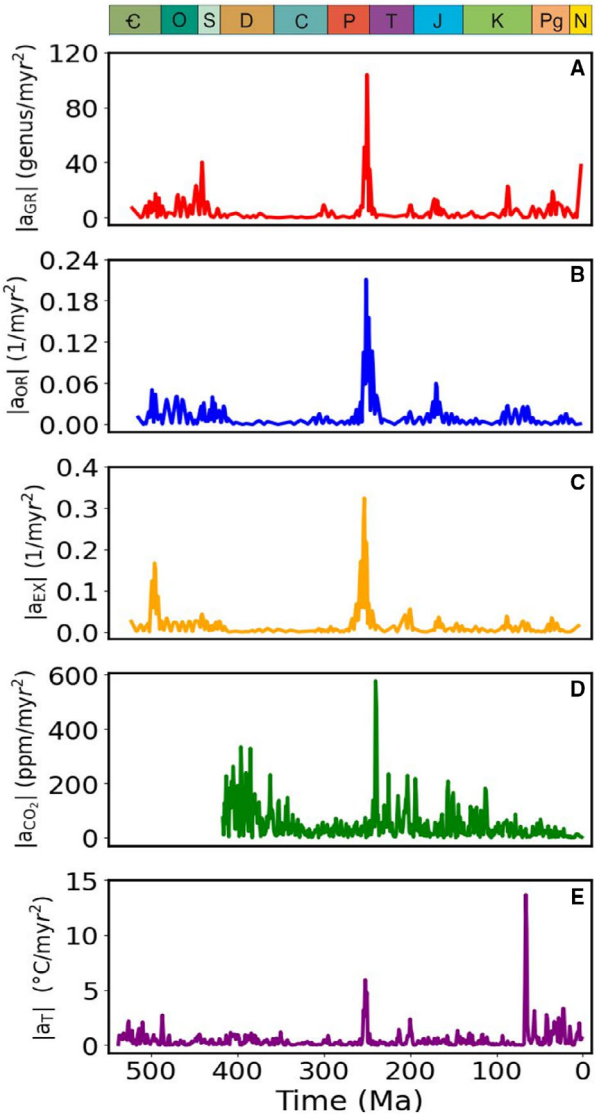


**FIG. 1.** Time series of the absolute values of the accelerations for five quantities characterizing the Phanerozoic biogeosystems: A, genus richness ($|a_{GR}|$); B, origination ($|a_{OR}|$); C, extinction ($|a_{EX}|$); D, atmospheric $CO_2$ level ($|a_{CO2}|$); E, global average temperature ($|a_T|$). Acceleration, *a*, is defined in the main text.

$R^2$, RMSE, and p-value from the KS test ($p_{KS}$) and CM test ($p_{CM}$) are presented in Tables 1 and 2. The $R^2$ values for the fitted power laws are close to 1 while the RMSE values are low, and the p-values of the KS and CM tests are all much larger than the critical value of 0.05 (Tables 1, 2). These results indicate that both pure and exponentially truncated power laws in Tables 1 and 2 fit the data points well.

While the scale-invariant patterns shown in Figure 2 and Tables 1 and 2, appear plausible, additional analyses are necessary to evaluate the performance of other heavy-tailed distributions including lognormal, exponential, and stretched-exponential distributions because random fluctuations may cause these distributions to resemble power-law-like patterns in the data (Clauset *et al.* 2009; Alstott *et al.* 2014). To test the goodness of fit of other heavy-tailed distributions compared to pure power laws and exponentially truncated power laws, I computed the BIC and conducted the LRT for these distributions (see Distribution Comparison & Selection, above). Table 3 presents the BIC values of the five distributions for the accelerations. For a given dataset, the distribution with the lowest BIC value is chosen as the best fit. According to the BIC values (Table 3), exponentially truncated power laws best fit the data in the categories of negative and all accelerations of genus richness (i.e. $|NA_{GR}|$ and $|AA_{GR}|$), negative accelerations of $CO_2$ (i.e. $|NA_{CO2}|$), and all accelerations of temperature (i.e. $|AA_T|$); for all other sets of accelerations, pure power laws offer the best fit. Tables 4–6 present the standardized likelihood ratios and their associated p-values of the LRTs for each pair of the five distributions. According to the results of LRTs (Tables 4–6), the pure or exponentially truncated power law outperforms the lognormal, exponential, and stretched-exponential distributions for all types of accelerations of the five quantities. For the positive accelerations of genus richness (i.e. $|PA_{GR}|$), negative and positive accelerations of origination (i.e. $|NA_{OR}|$ and $|PA_{OR}|$), positive and all accelerations of extinction (i.e. $|PA_{EX}|$ and $|AA_{EX}|$), as well as all accelerations of $CO_2$ (i.e. $|AA_{CO2}|$), the p-values of the LRTs for the exponentially truncated power law against the pure power law are greater than 0.05, implying that these LRTs are inconclusive. Therefore, both pure and exponentially truncated power laws could potentially offer plausible fits for these accelerations. The best-fitting distributions according to BIC values (Table 3) and LRTs (Tables 4–6) are summarized in Table 7. For some accelerations, the best-fitting distributions suggested by the BIC values differ from those indicated by the LRTs (Table 7). Due to the limited availability of data points, it is challenging to further determine whether these accelerations follow the pure or exponentially truncated power law. Future measurements of stratigraphic and fossil data with a higher resolution may help elaborate on this ambiguity.

The above results (Fig. 2; Tables 1—7) are based on the time series of the five quantities interpolated with the time step of 0.1 myr. To test whether the time step size influences the patterns in the accelerations, I interpolated the time series of the biological metrics and environmental variables with other time step sizes. As noted above, there exists a trade-off when choosing a proper time step size for the interpolation in this study. Here, I use 0.05 and 0.01 myr as the time steps to interpolate the time series of the five quantities and perform the same analyses. The statistical results for the accelerations of

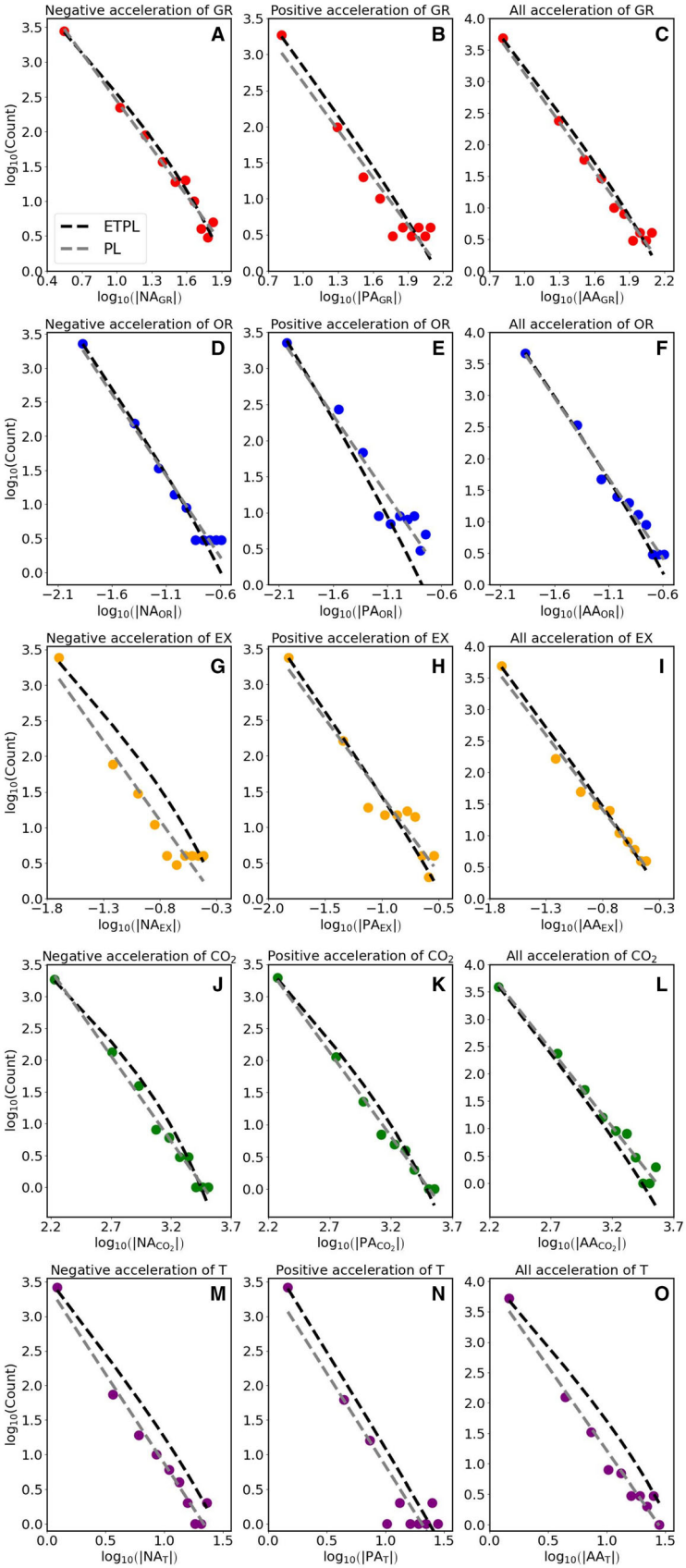

**FIG. 2.** Power law (PL) and exponentially truncated power law (ETPL) distributions of the negative acceleration (NA), positive acceleration (PA), and all acceleration (AA) of: A–C, genus richness (GR); D–F, origination (OR); G–I, extinction (EX); J–L, atmospheric $CO_2$ level ($CO_2$); M–O, global average temperature (T) during the Phanerozoic Eon. The time step between two consecutive data points in the interpolated time series is 0.1 myr. In each panel, the horizontal-axis value for each point is the logarithm of the midpoint of each bin for accelerations, the vertical-axis value for each point is the logarithm of the count in each bin for accelerations, and the black dashed curves and grey dashed lines are the best-fitting ETPL and PL distributions, respectively, for the points at the double logarithmic scale.

**TABLE 1.** Best-fitting power law (PL) distributions for negative acceleration (NA), positive acceleration (PA), and all acceleration (AA) of genus richness (GR), origination (OR), extinction (EX), atmospheric $CO_2$ level ($CO_2$), and global average temperature (T).

| Quantity | Category | Best-fitting PL | $R^2$ | RMSE | $p_{KS}$ | $p_{CM}$ |
|---|---|---|---|---|---|---|
| Acceleration of genus richness | $\lvert NA_{GR}\rvert = \{\lvert a_{GR}\rvert \mid a_{GR} < 0\}$ | $\text{Count} \sim \lvert NA_{GR}\rvert^{-2.28}$ | 0.98 | 0.12 | 1.00 | 1.00 |
| | $\lvert PA_{GR}\rvert = \{a_{GR} \mid a_{GR} > 0\}$ | $\text{Count} \sim \lvert PA_{GR}\rvert^{-2.20}$ | 0.93 | 0.23 | 0.79 | 0.68 |
| | $\lvert AA_{GR}\rvert = \{\lvert a_{GR}\rvert \mid a_{GR} \neq 0\}$ | $\text{Count} \sim \lvert AA_{GR}\rvert^{-2.58}$ | 0.98 | 0.14 | 0.99 | 0.97 |
| Acceleration of origination | $\lvert NA_{OR}\rvert = \{\lvert a_{OR}\rvert \mid a_{OR} < 0\}$ | $\text{Count} \sim \lvert NA_{OR}\rvert^{-2.39}$ | 0.97 | 0.15 | 0.79 | 0.54 |
| | $\lvert PA_{OR}\rvert = \{a_{OR} \mid a_{OR} > 0\}$ | $\text{Count} \sim \lvert PA_{OR}\rvert^{-2.22}$ | 0.93 | 0.23 | 0.78 | 0.68 |
| | $\lvert AA_{OR}\rvert = \{\lvert a_{OR}\rvert \mid a_{OR} \neq 0\}$ | $\text{Count} \sim \lvert AA_{OR}\rvert^{-2.54}$ | 0.99 | 0.12 | 0.99 | 0.97 |
| Acceleration of extinction | $\lvert NA_{EX}\rvert = \{\lvert a_{EX}\rvert \mid a_{EX} < 0\}$ | $\text{Count} \sim \lvert NA_{EX}\rvert^{-2.22}$ | 0.93 | 0.24 | 0.79 | 0.42 |
| | $\lvert PA_{EX}\rvert = \{a_{EX} \mid a_{EX} > 0\}$ | $\text{Count} \sim \lvert PA_{EX}\rvert^{-2.16}$ | 0.92 | 0.23 | 0.99 | 0.92 |
| | $\lvert AA_{EX}\rvert = \{\lvert a_{EX}\rvert \mid a_{EX} \neq 0\}$ | $\text{Count} \sim \lvert AA_{EX}\rvert^{-2.36}$ | 0.98 | 0.13 | 0.99 | 0.97 |
| Acceleration of $CO_2$ | $\lvert NA_{CO2}\rvert = \{\lvert a_{CO2}\rvert \mid a_{CO2} < 0\}$ | $\text{Count} \sim \lvert NA_{CO2}\rvert^{-2.68}$ | 0.99 | 0.11 | 0.99 | 0.92 |
| | $\lvert PA_{CO2}\rvert = \{a_{CO2} \mid a_{CO2} > 0\}$ | $\text{Count} \sim \lvert PA_{CO2}\rvert^{-2.63}$ | 0.99 | 0.08 | 1.00 | 0.99 |
| | $\lvert AA_{CO2}\rvert = \{\lvert a_{CO2}\rvert \mid a_{CO2} \neq 0\}$ | $\text{Count} \sim \lvert AA_{CO2}\rvert^{-2.83}$ | 0.98 | 0.16 | 0.99 | 0.97 |
| Acceleration of temperature | $\lvert NA_T\rvert = \{\lvert a_T\rvert \mid a_T < 0\}$ | $\text{Count} \sim \lvert NA_T\rvert^{-2.59}$ | 0.97 | 0.16 | 1.00 | 0.99 |
| | $\lvert PA_T\rvert = \{a_T \mid a_T > 0\}$ | $\text{Count} \sim \lvert PA_T\rvert^{-2.68}$ | 0.89 | 0.36 | 0.79 | 0.46 |
| | $\lvert AA_T\rvert = \{\lvert a_T\rvert \mid a_T \neq 0\}$ | $\text{Count} \sim \lvert AA_T\rvert^{-2.76}$ | 0.97 | 0.17 | 0.99 | 0.92 |

The time step between two consecutive data points in the interpolated time series of these five quantities is 0.1 myr.
Reported statistics include the coefficient of determination ($R^2$), root mean square error (RMSE), Kolmogorov–Smirnov test p-value ($p_{KS}$), and Cramér–von Mises test p-value ($p_{CM}$).

these new time series are presented in Figures S1−S3 and Tables S2−S5. These time series interpolated with 0.05 and 0.01 myr are used only for testing the sensitivity of the results to the time step size because attaining such high resolutions of the stratigraphic age is rather challenging in practice. The values of parameters in the best-fitting pure and exponentially truncated power laws for the time series interpolated with three different time step sizes (i.e. 0.1, 0.05 and 0.01 myr) are summarized in Tables 8 and 9, respectively. These results suggest that the parameter values of the pure or exponentially truncated power laws do not depend on the time step size used to interpolate the time series.

### *Temporal correlations*

To investigate the temporal correlations among these systematic pure and exponentially truncated power laws in the accelerations of the Phanerozoic biogeosystems, I calculated the Pearson's $r$ and Spearman's ρ among these accelerations. Since the accelerations neither follow the standard normal distribution nor approximate normality, the investigation here is informed mainly by the Spearman correlation analysis, which does not require the dataset to adhere to the normality assumption (Freedman 2009; McElreath 2018). The Spearman's ρ values among each pair of accelerations are presented in Table 10 and visualized in Figure 3, while the Pearson's $r$ values among each pair of accelerations are reported in Table S6 and Figure S3.

Among the ten pairs of accelerations, the Spearman's ρ for the accelerations of genus richness versus extinction (i.e. $a_{GR}$ vs $a_{EX}$ ) is 0.39 and the p -value is much less than 0.05 (appearing in the top half of Table 10), indicating that this pair of accelerations is positively correlated. Meanwhile, the Spearman's $\rho$ for the absolute values of these two accelerations (i.e. $|a_{GR}|$vs$|a_{EX}|$) is 0.31 and the p -value is again much smaller than 0.05 (appearing in the bottom half of Table 10), supporting the conclusion that the accelerations of genus richness and extinction are moderately correlated.

**TABLE 2.** Best-fitting exponentially truncated power law (ETPL) distributions for negative acceleration (NA), positive acceleration (PA), and all acceleration (AA) of genus richness (GR), origination (OR), extinction (EX), atmospheric $CO_2$ level ($CO_2$), and global average temperature (T).

| Quantity | Category | Best-fitting ETPL | $R^2$ | RMSE | $p_{KS}$ | $p_{CM}$ |
|---|---|---|---|---|---|---|
| Acceleration of genus richness | $\lvert NA_{GR}\rvert = \{\lvert a_{GR}\rvert \mid a_{GR} < 0\}$ | $\text{Count} \sim \exp(-0.02 \times \lvert NA_{GR}\rvert) \times \lvert NA_{GR}\rvert^{-1.79}$ | 0.99 | 0.02 | 1.00 | 1.00 |
| | $\lvert PA_{GR}\rvert = \{a_{GR} \mid a_{GR} > 0\}$ | $\text{Count} \sim \exp(-0.01 \times \lvert PA_{GR}\rvert) \times \lvert PA_{GR}\rvert^{-2.19}$ | 0.99 | 0.01 | 0.79 | 0.50 |
| | $\lvert AA_{GR}\rvert = \{\lvert a_{GR}\rvert \mid a_{GR} \neq 0\}$ | $\text{Count} \sim \exp(-0.01 \times \lvert AA_{GR}\rvert) \times \lvert AA_{GR}\rvert^{-2.33}$ | 0.99 | 0.01 | 0.99 | 0.97 |
| Acceleration of origination | $\lvert NA_{OR}\rvert = \{\lvert a_{OR}\rvert \mid a_{OR} < 0\}$ | $\text{Count} \sim \exp(-3.28 \times \lvert NA_{OR}\rvert) \times \lvert NA_{OR}\rvert^{-2.36}$ | 0.99 | 0.002 | 0.79 | 0.54 |
| | $\lvert PA_{OR}\rvert = \{a_{OR} \mid a_{OR} > 0\}$ | $\text{Count} \sim \exp(-4.08 \times \lvert PA_{OR}\rvert) \times \lvert PA_{OR}\rvert^{-2.49}$ | 0.98 | 0.02 | 0.42 | 0.25 |
| | $\lvert AA_{OR}\rvert = \{\lvert a_{OR}\rvert \mid a_{OR} \neq 0\}$ | $\text{Count} \sim \exp(-3.04 \times \lvert AA_{OR}\rvert) \times \lvert AA_{OR}\rvert^{-2.50}$ | 0.99 | 0.004 | 0.99 | 0.92 |
| Acceleration of extinction | $\lvert NA_{EX}\rvert = \{\lvert a_{EX}\rvert \mid a_{EX} < 0\}$ | $\text{Count} \sim \exp(-3.73 \times \lvert NA_{EX}\rvert) \times \lvert NA_{EX}\rvert^{-1.73}$ | 0.97 | 0.05 | 0.17 | 0.13 |
| | $\lvert PA_{EX}\rvert = \{a_{EX} \mid a_{EX} > 0\}$ | $\text{Count} \sim \exp(-1.60 \times \lvert PA_{EX}\rvert) \times \lvert PA_{EX}\rvert^{-2.29}$ | 0.99 | 0.03 | 0.42 | 0.25 |
| | $\lvert AA_{EX}\rvert = \{\lvert a_{EX}\rvert \mid a_{EX} \neq 0\}$ | $\text{Count} \sim \exp(-0.89 \times \lvert AA_{EX}\rvert) \times \lvert AA_{EX}\rvert^{-2.41}$ | 0.99 | 0.02 | 0.99 | 0.97 |
| Acceleration of $CO_2$ | $\lvert NA_{CO2}\rvert = \{\lvert a_{CO2}\rvert \mid a_{CO2} < 0\}$ | $\text{Count} \sim \exp(-0.001 \times \lvert NA_{CO2}\rvert) \times \lvert NA_{CO2}\rvert^{-1.73}$ | 0.99 | 0.02 | 0.99 | 0.86 |
| | $\lvert PA_{CO2}\rvert = \{a_{CO2} \mid a_{CO2} > 0\}$ | $\text{Count} \sim \exp(-0.0006 \times \lvert PA_{CO2}\rvert) \times \lvert PA_{CO2}\rvert^{-2.08}$ | 0.99 | 0.01 | 0.99 | 0.99 |
| | $\lvert AA_{CO2}\rvert = \{\lvert a_{CO2}\rvert \mid a_{CO2} \neq 0\}$ | $\text{Count} \sim \exp(-0.0003 \times \lvert AA_{CO2}\rvert) \times \lvert AA_{CO2}\rvert^{-2.81}$ | 0.99 | 0.01 | 0.79 | 0.63 |
| Acceleration of temperature | $\lvert NA_T\rvert = \{\lvert a_T\rvert \mid a_T < 0\}$ | $\text{Count} \sim \exp(-0.04 \times \lvert NA_T\rvert) \times \lvert NA_T\rvert^{-2.15}$ | 0.99 | 0.03 | 0.79 | 0.54 |
| | $\lvert PA_T\rvert = \{a_T \mid a_T > 0\}$ | $\text{Count} \sim \exp(-0.01 \times \lvert PA_T\rvert) \times \lvert PA_T\rvert^{-2.73}$ | 0.99 | 0.01 | 0.78 | 0.36 |
| | $\lvert AA_T\rvert = \{\lvert a_T\rvert \mid a_T \neq 0\}$ | $\text{Count} \sim \exp(-0.05 \times \lvert AA_T\rvert) \times \lvert AA_T\rvert^{-2.16}$ | 0.99 | 0.03 | 0.42 | 0.27 |

The time step between two consecutive data points in the interpolated time series of these five quantities is 0.1 myr.
Reported statistics include the coefficient of determination ($R^2$), root mean square error (RMSE), Kolmogorov–Smirnov test p-value (pKS), and Cramér–von Mises test p-value (pCM).

**TABLE 3.** The Bayesian information criterion (BIC) for exponentially truncated power law (ETPL), power law (PL), lognormal (LN), exponential (Exp), and stretched exponential (S-Exp) distributions for the data in the categories of negative acceleration (NA), positive acceleration (PA), and all acceleration (AA) of genus richness (GR), origination (OR), extinction (EX), atmospheric $CO_2$ level ($CO_2$), and global average temperature (T).

| Quantity | Category | BIC | | | | |
|---|---|---|---|---|---|---|
| | | ETPL | PL | LN | Exp | S-Exp |
| Acceleration of genus richness | $\lvert NA_{GR}\rvert$ | **6548.37** | 6587.57 | 6561.81 | 6895.77 | 6557.87 |
| | $\lvert PA_{GR}\rvert$ | 1386.24 | **1381.29** | 1387.74 | 1430.61 | 1387.60 |
| | $\lvert AA_{GR}\rvert$ | **5015.35** | 5015.64 | 5018.83 | 5198.47 | 5018.41 |
| Acceleration of origination | $\lvert NA_{OR}\rvert$ | −2104.23 | **−2108.43** | −2103.21 | −2013.88 | −2103.23 |
| | $\lvert PA_{OR}\rvert$ | −1693.29 | **−1698.42** | −1691.98 | −1641.43 | −1691.98 |
| | $\lvert AA_{OR}\rvert$ | −3536.56 | **−3540.48** | −3534.17 | −3393.41 | −3533.93 |
| Acceleration of extinction | $\lvert NA_{EX}\rvert$ | −296.74 | **−299.99** | −295.19 | −295.03 | −295.77 |
| | $\lvert PA_{EX}\rvert$ | −3072.78 | **−3076.85** | −3069.66 | −2849.00 | −3067.93 |
| | $\lvert AA_{EX}\rvert$ | −5592.28 | **−5597.69** | −5589.15 | −5124.13 | −5580.31 |
| Acceleration of $CO_2$ | $\lvert NA_{CO2}\rvert$ | **6983.65** | 7002.15 | 6984.79 | 7059.75 | 6983.88 |
| | $\lvert PA_{CO2}\rvert$ | 3925.18 | **3924.93** | 3925.82 | 3963.41 | 3925.56 |
| | $\lvert AA_{CO2}\rvert$ | 2381.54 | **2374.45** | 2382.28 | 2393.69 | 2382.26 |
| Acceleration of temperature | $\lvert NA_T\rvert$ | 1150.44 | **1147.92** | 1152.73 | 1301.58 | 1152.52 |
| | $\lvert PA_T\rvert$ | 365.75 | **358.04** | 365.91 | 383.50 | 366.36 |
| | $\lvert AA_T\rvert$ | **2562.82** | 2567.59 | 2564.67 | 2983.43 | 2564.24 |

**Bold** values indicate the minimum BIC in each row.

The Spearman's ρ for the accelerations of the other five pairs of quantities (genus richness vs origination ($a_{GR}$ vs $a_{OR}$ ); genus richness vs temperature ($a_{GR}$ vs $a_T$ ); origination vs extinction ($a_{OR}$ vs $a_{EX}$ ); origination vs temperature ($a_{OR}$ vs $a_T$ ); and extinction vs temperature ($a_{EX}$ vs $a_T$ )) are 0.1, −0.15, −0.22, 0.04 and −0.11, respectively; their p -values are all less than 0.05 (appearing in the top half of Table 10). Spearman's ρ for the absolute values of these five pairs of accelerations all have p -values that are smaller than 0.05 as well (appearing in

**TABLE 4.** Likelihood ratio tests (LRTs) of the power law (PL) distribution against the exponentially truncated power law (ETPL), lognormal (LN), exponential (Exp), and stretched-exponential (S-Exp) distributions for the negative acceleration (NA), positive acceleration (PA), and all acceleration (AA) of genus richness (GR), origination (OR), extinction (EX), atmospheric $CO_2$ level ($CO_2$), and global average temperature (T).

| Quantity | Category | *LRT*(PL, ETPL) | p(PL, ETPL) | *LRT*(PL, LN) | p(PL, LN) | *LRT*(PL, Exp) | p(PL, Exp) | *LRT*(PL, S-Exp) | p(PL, S-Exp) |
|---|---|---|---|---|---|---|---|---|---|
| Acceleration of genus richness | $\|NA_{GR}\|$ | **−23.64** | **≪0.05** | **−16.92** | **≪0.05** | **154.10** | **≪0.05** | **−18.91** | **≪0.05** |
| | $\|PA_{GR}\|$ | −1.33 | 0.10 | −0.58 | 0.42 | **24.66** | **≪0.05** | −0.65 | 0.49 |
| | $\|AA_{GR}\|$ | **−4.43** | **0.003** | −2.69 | 0.13 | **91.41** | **≪0.05** | 2.89 | 0.19 |
| Acceleration of origination | $\|NA_{OR}\|$ | −1.81 | 0.06 | −1.30 | 0.27 | **47.28** | **≪0.05** | −1.31 | 0.36 |
| | $\|PA_{OR}\|$ | −1.38 | 0.10 | −0.72 | 0.33 | **28.49** | **≪0.05** | −0.72 | 0.48 |
| | $\|AA_{OR}\|$ | **−2.31** | **0.03** | −1.12 | 0.26 | **73.53** | **≪0.05** | −0.99 | 0.52 |
| Acceleration of extinction | $\|NA_{EX}\|$ | **−2.30** | **0.03** | −1.53 | 0.19 | 2.48 | 0.48 | −1.82 | 0.18 |
| | $\|PA_{EX}\|$ | −1.90 | 0.05 | −0.34 | 0.49 | **113.92** | **≪0.05** | 0.52 | 0.74 |
| | $\|AA_{EX}\|$ | −1.57 | 0.08 | −0.01 | 0.90 | **236.78** | **≪0.05** | 4.41 | 0.07 |
| Acceleration of $CO_2$ | $\|NA_{CO2}\|$ | **−13.06** | **≪0.05** | **−12.49** | **0.002** | 28.79 | 0.07 | **−12.95** | **0.002** |
| | $\|PA_{CO2}\|$ | **−3.71** | **0.006** | −3.38 | 0.11 | 19.24 | 0.05 | −3.52 | 0.09 |
| | $\|AA_{CO2}\|$ | −0.62 | 0.26 | −0.25 | 0.60 | **9.61** | **0.03** | 0.27 | 0.93 |
| Acceleration of temperature | $\|NA_{T}\|$ | **−2.70** | **0.02** | −1.55 | 0.24 | **76.83** | **≪0.05** | −1.65 | 0.32 |
| | $\|PA_{T}\|$ | −0.09 | 0.67 | −0.006 | 0.92 | **12.73** | **0.009** | 0.22 | 0.71 |
| | $\|AA_{T}\|$ | **−6.69** | **≪0.05** | **−5.76** | **0.04** | **207.91** | **≪0.05** | **−5.97** | **0.04** |

The *LRT*(PL, ETPL), *LRT*(PL, LN), *LRT*(PL, Exp), and *LRT*(LN, S-Exp) represent the log-likelihood ratios for the PL distribution against the ETPL, LN, Exp, and S-Exp distributions, respectively, for each dataset. The p(PL, ETPL), p(PL, LN), p(PL, Exp), and p(LN, S-Exp) are the p-values for the statistical significance of these tests. **Bold** values indicate that the LRT results are statistically significant based on the associated p-values (i.e. when p-values are less than 0.05).

**TABLE 5.** Likelihood ratio tests (LRTs) of the exponentially truncated power law (ETPL) distribution against the lognormal (LN), exponential (Exp), and stretched-exponential (S-Exp) distributions for the negative acceleration (NA), positive acceleration (PA), and all acceleration (AA) of genus richness (GR), origination (OR), extinction (EX), atmospheric $CO_2$ level ($CO_2$), and global average temperature (T).

| Quantity | Category | *LRT*(ETPL, LN) | p(ETPL, LN) | *LRT*(ETPL, Exp) | p(ETPL, Exp) | *LRT*(ETPL, S-Exp) | p(ETPL, S-Exp) |
|---|---|---|---|---|---|---|---|
| Acceleration of genus richness | $\|NA_{GR}\|$ | **6.72** | **≪0.05** | **177.73** | **≪0.05** | **4.75** | **≪0.05** |
| | $\|PA_{GR}\|$ | **0.75** | **0.01** | **25.99** | **≪0.05** | **0.69** | **0.01** |
| | $\|AA_{GR}\|$ | **1.74** | **≪0.05** | **95.84** | **≪0.05** | **1.53** | **0.01** |
| Acceleration of origination | $\|NA_{OR}\|$ | 0.51 | 0.15 | **49.09** | **≪0.05** | 0.50 | 0.28 |
| | $\|PA_{OR}\|$ | **0.66** | **0.02** | **29.88** | **≪0.05** | 0.66 | 0.08 |
| | $\|AA_{OR}\|$ | **1.19** | **0.001** | **75.85** | **≪0.05** | **1.12** | **0.02** |
| Acceleration of extinction | $\|NA_{EX}\|$ | **0.78** | **0.02** | **4.79** | **0.03** | **0.48** | **0.01** |
| | $\|PA_{EX}\|$ | **1.56** | **≪0.05** | **115.82** | **≪0.05** | **2.42** | **≪0.05** |
| | $\|AA_{EX}\|$ | **1.53** | **0.03** | **238.35** | **≪0.05** | **5.98** | **≪0.05** |
| Acceleration of $CO_2$ | $\|NA_{CO2}\|$ | 0.57 | 0.60 | **41.86** | **≪0.05** | 0.11 | 0.87 |
| | $\|PA_{CO2}\|$ | 0.31 | 0.54 | **22.94** | **0.005** | 0.19 | 0.63 |
| | $\|AA_{CO2}\|$ | 10.24 | 0.63 | 0.008 | 0.26 | 0.37 | 0.07 |
| Acceleration of temperature | $\|NA_{T}\|$ | **1.14** | **0.008** | **79.52** | **≪0.05** | **1.04** | **0.04** |
| | $\|PA_{T}\|$ | 0.08 | 0.51 | **12.82** | **0.007** | 0.30 | 0.45 |
| | $\|AA_{T}\|$ | 0.92 | 0.31 | **214.59** | **≪0.05** | 0.71 | 0.42 |

The *LRT*(ETPL, LN), *LRT*(ETPL, Exp), and *LRT*(ETPL, S-Exp) represent the log-likelihood ratios for the ETPL distribution against the LN, Exp, and S-Exp distributions, respectively, for each dataset. The p(ETPL, LN), p(ETPL, Exp), and p(ETPL, S-Exp) are the p-values for the statistical significance of these tests. **Bold** values indicate that the LRT results are statistically significant based on the associated p-values (i.e. when p-values are less than 0.05).

**TABLE 6.** The likelihood ratio test (LRT) of the lognormal (LN) distribution against the exponential (Exp) and stretched-exponential (S-Exp) distributions as well as the LRT of the Exp distribution against the S-Exp distribution for the negative acceleration (NA), positive acceleration (PA), and all acceleration (AA) of genus richness (GR), origination (OR), extinction (EX), atmospheric $CO_2$ level ($CO_2$), and global average temperature (T).

| Quantity | Category | *LRT*(LN, Exp) | p(LN, Exp) | *LRT*(LN, S-Exp) | p(LN, S-Exp) | *LRT*(Exp, S-Exp) | p(Exp, S-Exp) |
|---|---|---|---|---|---|---|---|
| Acceleration of genus richness | $\lvert NA_{GR}\rvert$ | **171.02** | **≪0.05** | **−1.97** | **≪0.05** | **−172.99** | **≪0.05** |
| | $\lvert PA_{GR}\rvert$ | **25.23** | **≪0.05** | −0.07 | 0.76 | **−25.31** | **≪0.05** |
| | $\lvert AA_{GR}\rvert$ | **94.10** | **≪0.05** | −0.21 | 8.66 | **−94.31** | **≪0.05** |
| Acceleration of origination | $\lvert NA_{OR}\rvert$ | **48.57** | **≪0.05** | −0.01 | 0.96 | **−48.58** | **≪0.05** |
| | $\lvert PA_{OR}\rvert$ | **29.22** | **≪0.05** | −0.0008 | 0.99 | **−29.21** | **≪0.05** |
| | $\lvert AA_{OR}\rvert$ | **74.65** | **≪0.05** | 0.12 | 0.82 | **−74.53** | **≪0.05** |
| Acceleration of extinction | $\lvert NA_{EX}\rvert$ | 4.01 | 0.09 | −0.29 | 0.15 | **−4.30** | **0.003** |
| | $\lvert PA_{EX}\rvert$ | **114.26** | **≪0.05** | 0.86 | 0.41 | **−113.40** | **≪0.05** |
| | $\lvert AA_{EX}\rvert$ | **236.79** | **≪0.05** | 4.42 | 0.05 | **−232.37** | **≪0.05** |
| Acceleration of $CO_2$ | $\lvert NA_{CO2}\rvert$ | **41.29** | **≪0.05** | −0.46 | 0.27 | **−41.74** | **≪0.05** |
| | $\lvert PA_{CO2}\rvert$ | **22.63** | **≪0.05** | −0.13 | 0.38 | **−22.75** | **≪0.05** |
| | $\lvert AA_{CO2}\rvert$ | **9.87** | **0.01** | −0.01 | 0.97 | **9.88** | **≪0.05** |
| Acceleration of temperature | $\lvert NA_{T}\rvert$ | **78.38** | **≪0.05** | −0.11 | 0.79 | **−78.48** | **≪0.05** |
| | $\lvert PA_{T}\rvert$ | **12.74** | **≪0.05** | 0.22 | 0.66 | **−12.52** | **≪0.05** |
| | $\lvert AA_{T}\rvert$ | **213.68** | **≪0.05** | −0.22 | 0.34 | **−213.89** | **≪0.05** |

The *LRT*(LN, Exp) and *LRT*(LN, S-Exp) represent the log-likelihood ratios for the LN distribution against the Exp and S-Exp distributions, respectively, for each dataset. The *LRT*(Exp, S-Exp) represents the log-likelihood ratios for the Exp distribution against the S-Exp distribution for each dataset. The p(LN, Exp), p(Ln, S-Exp), and p(Exp, S-Exp) are the p-values for the statistical significance of these tests. **Bold** values indicate that the LRT results are statistically significant based on the associated p-values (i.e. when p-values are less than 0.05).

**TABLE 7.** Summary of the best-fitting distributions for the negative acceleration (NA), positive acceleration (PA), and all acceleration (AA) of genus richness (GR), origination (OR), extinction (EX), atmospheric $CO_2$ level ($CO_2$), and global average temperature (T).

| Quantity | Category | The best-fitting distribution based on LRT | The best-fitting distribution based on BIC | The best-fitting distribution |
|---|---|---|---|---|
| Acceleration of genus richness | $\lvert NA_{GR}\rvert$ | ETPL | ETPL | ETPL |
| | $\lvert PA_{GR}\rvert$ | Inconclusive | PL | PL |
| | $\lvert AA_{GR}\rvert$ | ETPL | ETPL | ETPL |
| Acceleration of origination | $\lvert NA_{OR}\rvert$ | Inconclusive | PL | PL |
| | $\lvert PA_{OR}\rvert$ | Inconclusive | PL | PL |
| | $\lvert AA_{OR}\rvert$ | ETPL | PL | ETPL or PL |
| Acceleration of extinction | $\lvert NA_{EX}\rvert$ | ETPL | PL | ETPL or PL |
| | $\lvert PA_{EX}\rvert$ | Inconclusive | PL | PL |
| | $\lvert AA_{EX}\rvert$ | Inconclusive | PL | PL |
| Acceleration of $CO_2$ | $\lvert NA_{CO2}\rvert$ | ETPL | ETPL | ETPL |
| | $\lvert PA_{CO2}\rvert$ | ETPL | PL | ETPL or PL |
| | $\lvert AA_{CO2}\rvert$ | Inconclusive | PL | PL |
| Acceleration of temperature | $\lvert NA_{T}\rvert$ | ETPL | PL | ETPL or PL |
| | $\lvert PA_{T}\rvert$ | ETPL | PL | ETPL or PL |
| | $\lvert AA_{T}\rvert$ | ETPL | ETPL | ETPL |

These best-fitting distributions are determined based on the likelihood ratio test (LRT) and Bayesian information criterion (BIC); the results of the LRT and BIC are presented in Tables 3–6. The PL and ETPL are the abbreviations of power law and exponentially truncated power law, respectively. The last column of this table summarizes the best-fitting distributions based on LRT and BIC. If the best-fitting distribution for a given dataset based on LRT is conclusive but differs from that based on BIC, then I conclude that 'ETPL or PL' is the best-fitting distribution. If the best-fitting distribution for a given dataset based on LRT is inconclusive, then I conclude that the best-fitting distribution based on BIC is the best-fitting distribution for this dataset.

**TABLE 8.** Summary of the exponent (α) of the power laws for the accelerations of genus richness (GR), origination (OR), extinction (EX), atmospheric $CO_2$ level ($CO_2$), and global average temperature (T).

| Quantity | Power law | Value of α | | |
|---|---|---|---|---|
| | | Step size = 0.1 myr | Step size = 0.05 myr | Step size = 0.01 myr |
| Acceleration of genus richness | Count ~ $\lvert NA_{GR}\rvert^{-\alpha}$ | 2.28 | 2.27 | 2.28 |
| | Count ~ $\lvert PA_{GR}\rvert^{-\alpha}$ | 2.20 | 2.21 | 2.22 |
| | Count ~ $\lvert AA_{GR}\rvert^{-\alpha}$ | 2.58 | 2.59 | 2.60 |
| Acceleration of origination | Count ~ $\lvert NA_{OR}\rvert^{-\alpha}$ | 2.39 | 2.39 | 2.39 |
| | Count ~ $\lvert PA_{OR}\rvert^{-\alpha}$ | 2.22 | 2.21 | 2.23 |
| | Count ~ $\lvert AA_{OR}\rvert^{-\alpha}$ | 2.54 | 2.54 | 2.55 |
| Acceleration of extinction | Count ~ $\lvert NA_{EX}\rvert^{-\alpha}$ | 2.22 | 2.22 | 2.23 |
| | Count ~ $\lvert PA_{EX}\rvert^{-\alpha}$ | 2.16 | 2.14 | 2.16 |
| | Count ~ $\lvert AA_{EX}\rvert^{-\alpha}$ | 2.36 | 2.35 | 2.37 |
| Acceleration of $CO_2$ | Count ~ $\lvert NA_{CO2}\rvert^{-\alpha}$ | 2.68 | 2.78 | 2.79 |
| | Count ~ $\lvert PA_{CO2}\rvert^{-\alpha}$ | 2.63 | 2.81 | 2.81 |
| | Count ~ $\lvert AA_{CO2}\rvert^{-\alpha}$ | 2.83 | 2.82 | 2.88 |
| Acceleration of temperature | Count ~ $\lvert NA_{T}\rvert^{-\alpha}$ | 2.59 | 2.64 | 2.62 |
| | Count ~ $\lvert PA_{T}\rvert^{-\alpha}$ | 2.68 | 2.68 | 2.67 |
| | Count ~ $\lvert AA_{T}\rvert^{-\alpha}$ | 2.76 | 2.74 | 2.75 |

The time series of these five quantities are interpolated with different time step sizes: 0.1, 0.05 and 0.01 myr. The statistical analyses of these power laws are presented in Tables 1, S2 and S4.

**TABLE 9.** Summary of the exponent (α) and cutoff parameter (λ) of the exponentially truncated power laws for the accelerations of genus richness (GR), origination (OR), extinction (EX), atmospheric $CO_2$ level ($CO_2$), and global average temperature (T).

| Quantity | Exponentially truncated power law | Value of (α, λ) | | |
|---|---|---|---|---|
| | | Step size = 0.1 myr | Step size = 0.05 myr | Step size = 0.01 myr |
| Acceleration of genus richness | Count ~ $\exp(-\lambda \times \lvert NA_{GR}\rvert) \times \lvert NA_{GR}\rvert^{-\alpha}$ | (1.79, 0.02) | (1.80, 0.02) | (1.65, 0.03) |
| | Count ~ $\exp(-\lambda \times \lvert PA_{GR}\rvert) \times \lvert PA_{GR}\rvert^{-\alpha}$ | (2.19, 0.01) | (2.20, 0.005) | (2.29, 0.004) |
| | Count ~ $\exp(-\lambda \times \lvert AA_{GR}\rvert) \times \lvert AA_{GR}\rvert^{-\alpha}$ | (2.33, 0.01) | (2.31, 0.009) | (2.30, 0.009) |
| Acceleration of origination | Count ~ $\exp(-\lambda \times \lvert NA_{OR}\rvert) \times \lvert NA_{OR}\rvert^{-\alpha}$ | (2.36, 3.28) | (2.35, 3.34) | (2.34, 3.49) |
| | Count ~ $\exp(-\lambda \times \lvert PA_{OR}\rvert) \times \lvert PA_{OR}\rvert^{-\alpha}$ | (2.49, 4.08) | (2.40, 4.82) | (2.38, 5.06) |
| | Count ~ $\exp(-\lambda \times \lvert AA_{OR}\rvert) \times \lvert AA_{OR}\rvert^{-\alpha}$ | (2.50, 3.04) | (2.49, 3.07) | (2.48, 3.19) |
| Acceleration of extinction | Count ~ $\exp(-\lambda \times \lvert NA_{EX}\rvert) \times \lvert NA_{EX}\rvert^{-\alpha}$ | (1.73, 3.73) | (1.77, 3.62) | (1.72, 3.78) |
| | Count ~ $\exp(-\lambda \times \lvert PA_{EX}\rvert) \times \lvert PA_{EX}\rvert^{-\alpha}$ | (2.29, 1.60) | (2.29, 1.59) | (2.29, 1.63) |
| | Count ~ $\exp(-\lambda \times \lvert AA_{EX}\rvert) \times \lvert AA_{EX}\rvert^{-\alpha}$ | (2.41, 0.89) | (2.40, 0.91) | (2.40, 0.91) |
| Acceleration of $CO_2$ | Count ~ $\exp(-\lambda \times \lvert NA_{CO2}\rvert) \times \lvert NA_{CO2}\rvert^{-\alpha}$ | (1.73, 0.001) | (2.96, 0.0004) | (2.68, 0.0004) |
| | Count ~ $\exp(-\lambda \times \lvert PA_{CO2}\rvert) \times \lvert PA_{CO2}\rvert^{-\alpha}$ | (2.08, 0.0006) | (2.62, 0.0003) | (2.63, 0.0003) |
| | Count ~ $\exp(-\lambda \times \lvert AA_{CO2}\rvert) \times \lvert AA_{CO2}\rvert^{-\alpha}$ | (2.81, 0.0003) | (2.70, 0.0003) | (2.63, 0.0004) |
| Acceleration of temperature | Count ~ $\exp(-\lambda \times \lvert NA_{T}\rvert) \times \lvert NA_{T}\rvert^{-\alpha}$ | (2.15, 0.04) | (2.13, 0.04) | (2.12, 0.04) |
| | Count ~ $\exp(-\lambda \times \lvert PA_{T}\rvert) \times \lvert PA_{T}\rvert^{-\alpha}$ | (2.73, 0.01) | (2.49, 0.02) | (2.47, 0.03) |
| | Count ~ $\exp(-\lambda \times \lvert AA_{T}\rvert) \times \lvert AA_{T}\rvert^{-\alpha}$ | (2.16, 0.05) | (2.30, 0.04) | (2.28, 0.04) |

The time series of these five quantities are interpolated with different time step sizes: 0.1, 0.05 and 0.01 myr. The statistical analyses of these exponentially truncated power laws are presented in Tables 2, S3 and S5.

the bottom half of Table 10). These findings indicate that each of these five pairs of accelerations is weakly correlated, with the correlation between the accelerations of origination and temperature being especially insignificant.

For the remaining four pairs of quantities, including genus richness versus $CO_2$ (i.e. $a_{GR}$ vs $a_{CO2}$), origination versus $CO_2$ (i.e. $a_{OR}$ vs $a_{CO2}$), extinction versus $CO_2$ (i.e. $a_{EX}$ vs $a_{CO2}$), and temperature versus $CO_2$ (i.e. $a_T$ vs $a_{CO2}$),

**TABLE 10.** Summary of the Spearman's rank correlation coefficient values (Spearman's ρ) and p-values ($p_\rho$) for the accelerations of each pair of variables ($a_{GR}$, $a_{OR}$, $a_{EX}$, $a_{CO2}$, and $a_T$) and the absolute values of these accelerations ($|a_{GR}|$, $|a_{OR}|$, $|a_{EX}|$, $|a_{CO2}|$, and $|a_T|$).

| Quantity | Variable pair | Spearman's ρ | $p_\rho$ |
|---|---|---|---|
| Accelerations of biological metrics and environmental variables | $a_{GR}$ vs $a_{OR}$ | **0.10** | **0.04** |
| | $a_{GR}$ vs $a_{EX}$ | **0.39** | **≪0.05** |
| | $a_{GR}$ vs $a_{CO2}$ | 0.02 | 0.62 |
| | $a_{GR}$ vs $a_T$ | **−0.15** | **≪0.05** |
| | $a_{OR}$ vs $a_{EX}$ | **−0.22** | **≪0.05** |
| | $a_{OR}$ vs $a_{CO2}$ | 0.05 | 0.34 |
| | $a_{OR}$ vs $a_T$ | **0.04** | **≪0.05** |
| | $a_{EX}$ vs $a_{CO2}$ | −0.01 | 0.90 |
| | $a_{EX}$ vs $a_T$ | **−0.11** | **0.03** |
| | $a_{CO2}$ vs $a_T$ | 0.07 | 0.14 |
| Absolute values of the accelerations of biological metrics and environmental variables | $\|a_{GR}\|$ vs $\|a_{OR}\|$ | **0.36** | **≪0.05** |
| | $\|a_{GR}\|$ vs $\|a_{EX}\|$ | **0.31** | **≪0.05** |
| | $\|a_{GR}\|$ vs $\|a_{CO2}\|$ | −0.04 | 0.48 |
| | $\|a_{GR}\|$ vs $\|a_T\|$ | **0.19** | **≪0.05** |
| | $\|a_{OR}\|$ vs $\|a_{EX}\|$ | **0.38** | **≪0.05** |
| | $\|a_{OR}\|$ vs $\|a_{CO2}\|$ | −0.05 | 0.25 |
| | $\|a_{OR}\|$ vs $\|a_T\|$ | **−0.005** | **0.02** |
| | $\|a_{EX}\|$ vs $\|a_{CO2}\|$ | −0.01 | 0.87 |
| | $\|a_{EX}\|$ vs $\|a_T\|$ | **0.03** | **≪0.05** |
| | $\|a_{CO2}\|$ vs $\|a_T\|$ | −0.01 | 0.99 |

These Spearman's ρ values are visualized in Figure 3. **Bold** values indicate that the Spearman's ρ values are statistically significant based on the associated p-values (i.e. when p-values are less than 0.05). The Pearson correlation coefficient values (Pearson's *r*) and p-values ($p_r$) for these accelerations are presented in Table S6 and Figure S3. Note that the analysis and discussion about the temporal correlations among these accelerations are primarily based on Spearman's ρ values because these accelerations are neither the standard normal distribution nor approximately normally distributed (see Correlation Analysis).

the p -values of their Spearman's ρ are all much greater than 0.05 (appearing in the top half of Table 10). Moreover, the p -values of the Spearman's ρ for the absolute values of these four pairs of accelerations are also all much larger than 0.05 (appearing in the bottom half of Table 10). These results imply that these four pairs of accelerations are uncorrelated.

It is well-known that environmental changes can exert selection pressures on organisms and impact the evolutionary trajectories of biological systems (Erwin 2009; Condamine *et al.* 2013). Here, I explore whether the accelerations of the three biological metrics are correlated with the two environmental variables or their variation rates, analogous to the relation between the acceleration and external force stated in Newton's second law. The Spearman's ρ values obtained from these correlation analyses are presented in Table 11, while the Pearson's *r* values are presented in Table S7. The Spearman's ρ for the acceleration of genus richness versus the variable $CO_2$ (i.e. $a_{GR}$ vs $CO_2$) is −0.10 and the p-value is less than 0.05 (appearing in the top half of Table 11), suggesting that they are weakly correlated. The Spearman's ρ for the other five pairs of biological metrics' accelerations versus environmental variables (appearing in the top half of Table 11) are all much greater than 0.05, indicating that these accelerations are not affected by either $CO_2$ or temperature. The relations among biological metrics' accelerations and environmental variables' variation rates are different. The Spearman's ρ for the acceleration of origination versus the variation rate of temperature (i.e. $a_{OR}$ vs $R_T$) and the acceleration of extinction versus the variation rate of temperature (i.e. $a_{EX}$ vs $R_T$) are 0.17 and −0.10, respectively, and their p-values are less than 0.05 (appearing in the bottom half of Table 11), implying that these two pairs of quantities are weakly correlated and

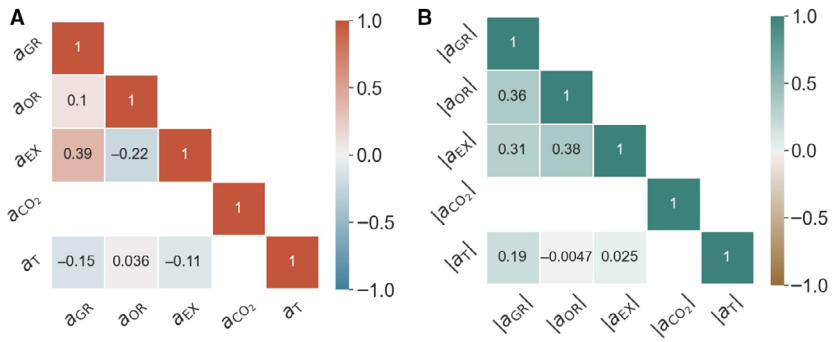


**FIG. 3.** A, heatmap of the Spearman's rank correlation coefficient values (Spearman's ρ) for the accelerations (*a*) of genus richness (GR), origination (OR), extinction (EX), atmospheric $CO_2$ level ($CO_2$), and global average temperature (T); the accelerations of these five quantities are denoted as $a_{GR}$, $a_{OR}$, $a_{EX}$, $a_{CO2}$, and $a_T$, respectively. B, heatmap of the Spearman's ρ values for the absolute values of the accelerations of these five quantities ($|a_{GR}|$, $|a_{OR}|$, $|a_{EX}|$, $|a_{CO2}|$, and $|a_T|$). A blank cell in the lower triangle in both panels indicates that the p-value of the Spearman's ρ for that pair of accelerations represented by this cell is greater than 0.05 and therefore this Spearman's ρ value is not statistically significant.

**TABLE 11.** Summary of the Spearman's rank correlation coefficient values (Spearman's ρ) and p-values ($p_\rho$) for: (1) biological metrics' accelerations ($a_{GR}$, $a_{OR}$, and $a_{EX}$) versus environmental variables ($CO_2$ and T), and (2) biological metrics' accelerations ($a_{GR}$, $a_{OR}$, and $a_{EX}$) versus environmental variables' variation rates ($R_{CO2}$ and $R_T$).

| Quantity | Variable pair | Spearman's ρ | $p_\rho$ |
|---|---|---|---|
| Biological metrics' accelerations vs environmental variables | $a_{GR}$ vs $CO_2$ | **−0.10** | **0.03** |
| | $a_{GR}$ vs T | −0.0002 | 0.99 |
| | $a_{OR}$ vs $CO_2$ | 0.001 | 0.98 |
| | $a_{OR}$ vs T | 0.01 | 0.83 |
| | $a_{EX}$ vs $CO_2$ | −0.03 | 0.52 |
| | $a_{EX}$ vs T | −0.001 | 0.97 |
| Biological metrics' accelerations vs environmental variables' variation rates | $a_{GR}$ vs $R_{CO_2}$ | −0.03 | 0.61 |
| | $a_{GR}$ vs $R_T$ | 0.04 | 0.45 |
| | $a_{OR}$ vs $R_{CO_2}$ | 0.01 | 0.88 |
| | $a_{OR}$ vs $R_T$ | **0.17** | **$\ll$0.05** |
| | $a_{EX}$ vs $R_{CO_2}$ | −0.06 | 0.22 |
| | $a_{EX}$ vs $R_T$ | **−0.10** | **0.04** |

The purpose of investigating the correlations among these quantities is to explore whether environmental changes may exert selection pressures on organisms and influence the accelerations of the biological metrics. **Bold** values indicate that the Spearman's ρ values are statistically significant based on the associated p-values (i.e. when p-values are less than 0.05). The Pearson correlation coefficient values (Pearson's $r$) and p-values ($p_r$) for these quantities are presented in Table S7. Note that the analysis and discussion about the temporal correlations among these quantities are primarily based on Spearman's ρ values because these variables and their variation rates and accelerations are neither the standard normal distribution nor approximately normally distributed (see Correlation Analysis).

that the variation rate of temperature is likely to have influenced the accelerations of origination and extinction to a certain extent. The p-values of Spearman's ρ for the other four pairs of biological metrics' accelerations versus environmental variables' variation rates (appearing in the bottom half of Table 11) are all much greater than 0.05, indicating that no correlation exists among these accelerations and variation rates.

### *Implications*

Palaeobiological and geochemical studies have dedicated enormous efforts to reconstructing the biological metrics and environmental variables over geologic time through analysing fossil records and sedimentary rocks (Simpson 1944; Foote 2000; Sepkoski 2002; Alroy *et al.* 2008; Foster *et al.* 2017; Fan *et al.* 2020; Scotese *et al.* 2021). With the reconstructed and compiled datasets on these quantities, a variety of global-scale mathematical models (Lenton *et al.* 2018; Haywood *et al.* 2019; Mills *et al.* 2021) have been developed to investigate the evolutionary trajectories of biogeosystems. However, these studies generally focus on the time series of biological metrics and environmental variables as well as their variations; the accelerations of these quantities have seldom been studied. This work explores the evolutionary modes and dynamical patterns in the accelerations of five quantities characterizing the Phanerozoic biogeosystems and shows that these accelerations systematically exhibit scale-invariant patterns (Fig. 2; Tables 1, 2).

Similar to many complex systems possessing scale-invariant behaviours, the fundamental reasons for these scale-invariant accelerations appearing in the Phanerozoic biogeosystems remain unclear. From the view of nonlinear dynamics, studies have attributed scale-invariant patterns identified in a variety of natural systems to self-organized criticality. The concept of self-organized criticality, originally proposed by Bak *et al.* (1987), refers to the phenomenon that the internal interactions of a large system self-organize it into states at which scale-invariant patterns appear. When stepping into critical points, nonlinear systems with self-organized criticality exhibit scale-invariant sizes/durations and the $1/f$ power spectra (Bak *et al.* 1987). It has been suggested that the best-known scale-invariant pattern on the ancient Earth (i.e. the power law in the frequency vs size of extinction events in the Phanerozoic) originated from self-organized critical evolutionary dynamics (Bak & Sneppen 1993; Sole *et al.* 1997). Nevertheless, the scale-invariant behaviour, as an emergent property of self-organized criticality, does not necessarily derive from the latter (Hergarten 2002; Marković & Gros 2014). Some studies (Newman 1996; Kirchner & Weil 1998; Newman & Eble 1999; Plotnick & Sepkoski 2001; Yacobucci 2005) have argued against the existence of self-organized criticality in the Phanerozoic evolutionary processes. After all, research on the connection between scale invariance and self-organized criticality generally relies on numerical simulations; no common and definite interpretation exists for such a connection (Hergarten 2002; Marković & Gros 2014). Whether the scale-invariant accelerations reported in this study are related to self-organized criticality remains unknown.

The distributions of accelerations (Fig. 2) show that the frequency of the occurrence of extreme accelerations is much lower than that of small ones, implying that Phanerozoic biogeosystems might have been stabilized at certain equilibria during most time intervals (Payne *et al.* 2020). With the evolution of Earth's surface environments and the emergence of new species across the Phanerozoic Eon (Alroy *et al.* 2008; Benson *et al.* 2021; Shaviv *et al.* 2023), the complexity of biogeosystems elevated, leading to strong resilience to environmental perturbations and preventing biogeosystems from heading

toward crises in many cases (Lenton & Watson 2013; Lovelock 2016). Moreover, the extreme accelerations, which contribute to the right tails of the scale-invariant patterns in Figure 2, do not necessarily derive from external disturbances (Levin 1998; Lovelock 2016). While external forces can affect biological and geological evolution, they usually influence the Earth–life system by altering its degrees of freedom instead of directly triggering extreme variations (Jacobson *et al.* 2000; Steffen *et al.* 2005). Rather, the internal interactions of coupled components of the global biogeosystem and the integrated effects of various feedback mechanisms in Earth's surface environments can result in positive feedback loops that drive the system itself to evolve across critical states where extreme events may arise (Prigogine 1980; Vermeij 2024). For example, studies have suggested that dramatic transitions in life evolution (Crespi 2004; DeAngelis *et al.* 2012; Sudakov *et al.* 2017) and swift changes in geological environments and records (Scheffer *et al.* 2006; Gulick *et al.* 2017; Shang 2023b, 2023c) might have originated from positive feedback mechanisms that were amplified by internal interactions of biogeosystems. Similarly, certain positive feedback mechanisms might also have been responsible for the extreme accelerations in Phanerozoic biogeosystems. For instance, the extinction of some groups of species in a biological system could lead to the reorganization of ecological networks (Rudolf & Lafferty 2011; Muscente *et al.* 2018). The failure of such a reorganization to a new balanced state would shift the biological system to a critical point at which larger extinction would occur, resulting in automatic collapse (Plotnick & McKinney 1993; Sneppen *et al.* 1995); this process is also referred to as the secondary extinction (Eklöf & Ebenman 2006; Brodie *et al.* 2014). Such a positive feedback loop (i.e. an initial small extinction eventually evolving to severe collapse) probably contributed to the extreme accelerations of extinction shown in this study.

The results here have several implications for the studies of biological and geological evolution. First, scale-invariant accelerations systematically appeared in the Phanerozoic biogeosystems, suggesting that such patterns may not be limited to the five quantities investigated in this work. Instead, they probably also exist in other metrics, such as the diversification of species (Alroy 2010; Morlon 2014; Foote 2023); exploring the accelerations in these quantities may enrich our understanding of the evolutionary processes and dynamical properties of biogeosystems. Moreover, this study shows that extreme events are crucial components of the scale-invariant accelerations (i.e. the right tails on the log–log plots in Fig. 2). The scale-invariant behaviours in other quantities characterizing the evolution of biogeosystems may remain concealed because extreme events have been considered outliers and removed prior to statistical analysis. Cautious evaluations of the seemingly unusual data points (e.g. extreme events) are important for uncovering the dynamical patterns of biogeosystems. Furthermore, as mentioned above, the extreme accelerations presented in this work might have derived from the internal interactions of coupled components and interlocked feedback mechanisms, rather than only from external disturbances, implying that the studies on the evolution of biogeosystems should focus more on intrinsic interactions rather than solely on external perturbations. Leveraging these internal interactions and the self-regulating capacities of biogeosystems in sustainable practices would facilitate the evolution of the Earth-life system along a relatively stable trajectory in the future.

*Acknowledgements.* I thank Editors Bethany Allen and Sally Thomas for valuable suggestions. I am grateful to William Gearty and other anonymous reviewers for thoughtful and constructive comments. This work is supported by a start-up fund from The University of Texas at El Paso and a research fund award from the International Association for Mathematical Geosciences.

## DATA ARCHIVING STATEMENT

Code for this study is available on GitHub: https://github.com/Shang-Research/Accelerations-of-the-Phanerozoic-Biogeosystems.

*Editor.* Bethany Allen

## SUPPORTING INFORMATION

Additional Supporting Information can be found online (https://doi.org/10.1111/pala.12734):

**Table S1.** Metadata of original datasets.
**Table S2.** Best-fitting power law distributions for negative acceleration, positive acceleration, and all acceleration of genus richness, origination, extinction, atmospheric $CO_2$ level, and global average temperature. Time series of these five quantities are interpolated with the time step of 0.05 myr.
**Table S3.** Best-fitting exponentially truncated power law distributions for negative acceleration, positive acceleration, and all acceleration of genus richness, origination, extinction, atmospheric $CO_2$ level, and global average temperature. Time series of these five quantities are interpolated with the time step of 0.05 myr.
**Table S4.** Best-fitting power law distributions for negative acceleration, positive acceleration, and all acceleration of genus richness, origination, extinction, atmospheric $CO_2$ level, and global average temperature. Time series of these five quantities are interpolated with the time step of 0.01 myr.
**Table S5.** Best-fitting exponentially truncated power law distributions for negative acceleration, positive acceleration, and all acceleration of genus richness, origination, extinction, atmospheric $CO_2$ level, and global average temperature. Time series

of these five quantities are interpolated with the time step of 0.01 myr.

**Table S6.** Summary of the Pearson correlation coefficient values and p-values for (1) the accelerations of genus richness, origination, extinction, atmospheric $CO_2$ level, and global average temperature, and (2) the absolute values of these accelerations.

**Table S7.** Summary of the Pearson correlation coefficient values and p-value for (1) biological metrics' accelerations versus environmental variables, and (2) biological metrics' accelerations versus environmental variables' variation rates.

**Figure S1.** Power law and exponentially truncated power law distributions of the negative acceleration, positive acceleration, and all acceleration of genus richness, origination, extinction, atmospheric $CO_2$ level, and global average temperature. Time series of these five quantities are interpolated with the time step of 0.05 myr.

**Figure S2.** Power law and exponentially truncated power law distributions of the negative acceleration, positive acceleration, and all acceleration of genus richness, origination, extinction, atmospheric $CO_2$ level, and global average temperature. Time series of these five quantities are interpolated with the time step of 0.01 myr.

**Figure S3.** Heatmaps of the Pearson correlation coefficient values for (1) the accelerations of genus richness, origination, extinction, atmospheric $CO_2$ level, and global average temperature, and (2) the absolute values of these accelerations.

## REFERENCES


Alroy, J. 2010. Geographical, environmental and intrinsic biotic controls on Phanerozoic marine diversification. *Palaeontology*, **53** (6), 1211–1235.

Alroy, J., Aberhan, M., Bottjer, D. J., Foote, M., Fursich, F. T., Harries, P. J., Hendy, A. J., Holland, S. M., Ivany, L. C., Kiessling, W., Kosnik, M. A., Marshall, C. R., McGowan, A., Miller, A. I., Olszewski, T. D., Patzkowsky, M. E., Peters, S. E., Villier, L., Wagner, P. J., Bonuso, N., Borkow, P. S., Brenneis, B., Clapham, M. E., Fall, L. M., Ferguson, C. A., Hanson, V. L., Krug, A. Z., Layou, K. M., Leckey, E. H., Nürnberg, S., Powers, C. M., Sessa, J. A., Simpson, C., Tomasovych, A. and Visaggi, C. C. 2008. Phanerozoic trends in the global diversity of marine invertebrates. *Science*, **321** (5885), 97–100.

Alstott, J., Bullmore, E. and Plenz, D. 2014. Powerlaw: a Python package for analysis of heavy-tailed distributions. *PLoS One*, **9** (1), e85777.

Anderson, T. W. 1962. On the distribution of the two-sample Cramér-von Mises criterion. *The Annals of Mathematical Statistics*, **33** (3), 1148–1159.

Asmussen, S. 2003. *Applied probability and queues*. Springer.

Bak, P. and Sneppen, K. 1993. Punctuated equilibrium and criticality in a simple model of evolution. *Physical Review Letters*, **71** (24), 4083.

Bak, P., Tang, C. and Wiesenfeld, K. 1987. Self-organized criticality: an explanation of the *1/f* noise. *Physical Review Letters*, **59** (4), 381.

Bambach, R. K. 2006. Phanerozoic biodiversity mass extinctions. *Annual Review of Earth and Planetary Sciences*, **34**, 127–155.

Benson, R. B., Butler, R., Close, R. A., Saupe, E. and Rabosky, D. L. 2021. Biodiversity across space and time in the fossil record. *Current Biology*, **31** (19), R1225–R1236.

Blount, Z. D., Lenski, R. E. and Losos, J. B. 2018. Contingency and determinism in evolution: replaying life's tape. *Science*, **362** (6415), eaam5979.

Bond, D. P. and Grasby, S. E. 2017. On the causes of mass extinctions. *Palaeogeography, Palaeoclimatology, Palaeoecology*, **478**, 3–29.

Brodie, J. F., Aslan, C. E., Rogers, H. S., Redford, K. H., Maron, J. L., Bronstein, J. L. and Groves, C. R. 2014. Secondary extinctions of biodiversity. *Trends in Ecology & Evolution*, **29** (12), 664–672.

Bryson, M. C. 1974. Heavy-tailed distributions: properties and tests. *Technometrics*, **16** (1), 61–68.

Buse, A. 1982. The likelihood ratio, Wald, and Lagrange multiplier tests: an expository note. *The American Statistician*, **36** (3a), 153–157.

Cardinale, B. J., Duffy, J. E., Gonzalez, A., Hooper, D. U., Perrings, C., Venail, P., Narwani, A., Mace, G. M., Tilman, D., Wardle, D. A., Kinzig, A. P., Daily, G. C., Loreau, M., Grace, J. B., Larigauderie, A., Srivastava, D. S. and Naeem, S. 2012. Biodiversity loss and its impact on humanity. *Nature*, **486** (7401), 59–67.

Carlson, J. M. and Doyle, J. 1999. Highly optimized tolerance: a mechanism for power laws in designed systems. *Physical Review E*, **60** (2), 1412.

Clauset, A., Shalizi, C. R. and Newman, M. E. 2009. Power-law distributions in empirical data. *SIAM Review*, **51** (4), 661–703.

Condamine, F. L., Rolland, J. and Morlon, H. 2013. Macroevolutionary perspectives to environmental change. *Ecology Letters*, **16**, 72–85.

Crespi, B. J. 2004. Vicious circles: positive feedback in major evolutionary and ecological transitions. *Trends in Ecology & Evolution*, **19** (12), 627–633.

DeAngelis, D. L., Post, W. M. and Travis, C. C. 2012. *Positive feedback in natural systems*. Springer Science & Business Media.

Deluca, A. and Corral, Á. 2013. Fitting and goodness-of-fit test of non-truncated and truncated power-law distributions. *Acta Geophysica*, **61**, 1351–1394.

Deutsch, C., Ferrel, A., Seibel, B., Pörtner, H.-O. and Huey, R. B. 2015. Climate change tightens a metabolic constraint on marine habitats. *Science*, **348** (6239), 1132–1135.

Duran-Nebreda, S., Bentley, R. A., Vidiella, B., Spiridonov, A., Eldredge, N., O'Brien, M. J. and Valverde, S. 2024. On the multiscale dynamics of punctuated evolution. *Trends in Ecology & Evolution*, **39** (8), 734–744.

Eklöf, A. and Ebenman, B. O. 2006. Species loss and secondary extinctions in simple and complex model communities. *Journal of Animal Ecology*, **75** (1), 239–246.

Erwin, D. H. 2009. Climate as a driver of evolutionary change. *Current Biology*, **19** (14), R575–R583.

Fan, J. X., Shen, S. Z., Erwin, D. H., Sadler, P. M., Macleod, N., Cheng, A.-M., Hou, X.-D., Yang, J., Wang, X.-D., Wang, Y., Zhang, H., Chen, X., Li, G.-X., Zhang, Y. C., Shi, Y.-K., Yuan, D.-X., Chen, Q., Zhang, L.-N., Li, C. and Zhao, Y.-Y. 2020. A high-resolution summary of Cambrian to Early Triassic marine invertebrate biodiversity. *Science*, **367** (6475), 272–277.

Fitch, W. M. and Ayala, F. J. 1995. *Tempo and mode in evolution: Genetics and paleontology 50 years after Simpson*. National Academies Press.

Foote, M. 2000. Origination and extinction components of taxonomic diversity: general problems. *Paleobiology*, **26** (S4), 74–102.

Foote, M. 2023. Diversity-dependent diversification in the history of marine animals. *The American Naturalist*, **201** (5), 680–693.

Forbes, C., Evans, M., Hastings, N. and Peacock, B. 2011. *Statistical distributions*. John Wiley & Sons.

Foster, G. L. and Rohling, E. J. 2013. Relationship between sea level and climate forcing by $CO_2$ on geological timescales. *Proceedings of the National Academy of Sciences*, **110** (4), 1209–1214.

Foster, G. L., Royer, D. L. and Lunt, D. J. 2017. Future climate forcing potentially without precedent in the last 420 million years. *Nature Communications*, **8**, 14845.

Freedman, D. A. 2009. *Statistical models: Theory and practice*. Cambridge University Press.

Freund, R. J. and Wilson, W. J. 2003. *Statistical methods*. Elsevier.

Glazier, D. S. 2005. Beyond the "3/4-power law": variation in the intra-and interspecific scaling of metabolic rate in animals. *Biological Reviews*, **80** (4), 611–662.

Gould, S. J. 2002. *The structure of evolutionary theory*. Harvard University Press.

Gould, S. J. and Eldredge, N. 1977. Punctuated equilibria: the tempo and mode of evolution reconsidered. *Paleobiology*, **3** (2), 115–151.

Gulick, S. P., Shevenell, A. E., Montelli, A., Fernandez, R., Smith, C., Warny, S., Bohaty, S. M., Sjunneskog, C., Leventer, A., Frederick, B. and Blankenship, D. D. 2017. Initiation and long-term instability of the East Antarctic Ice Sheet. *Nature*, **552** (7684), 225–229.

Hannisdal, B. and Peters, S. E. 2011. Phanerozoic Earth system evolution and marine biodiversity. *Science*, **334** (6059), 1121–1124.

Haywood, A. M., Valdes, P. J., Aze, T., Barlow, N., Burke, A., Dolan, A. M., von der Heydt, A., Hill, D. J., Jamieson, S. S., Otto-Bliesner, B. L., Salzmann, U., Saupe, E. and Voss, J. 2019. What can palaeoclimate modelling do for you? *Earth Systems and Environment*, **3**, 1–18.

Hergarten, S. 2002. *Self-organized criticality in Earth systems. Vol. 2*. Springer.

Hooper, D. U., Adair, E. C., Cardinale, B. J., Byrnes, J. E., Hungate, B. A., Matulich, K. L., Gonzalez, A., Duffy, J. E., Gamfeldt, L. and O'Connor, M. I. 2012. A global synthesis reveals biodiversity loss as a major driver of ecosystem change. *Nature*, **486** (7401), 105–108.

Jacobson, M., Charlson, R. J., Rodhe, H. and Orians, G. H. 2000. *Earth system science: From biogeochemical cycles to global changes*. Academic Press.

Kirchner, J. W. and Weil, A. 1998. No fractals in fossil extinction statistics. *Nature*, **395** (6700), 337–338.

Kocsis, Á. T., Reddin, C. J., Alroy, J. and Kiessling, W. 2019. The R package divDyn for quantifying diversity dynamics using fossil sampling data. *Methods in Ecology and Evolution*, **10** (5), 735–743.

Lenton, T. and Watson, A. 2013. *Revolutions that made the Earth*. Oxford University Press.

Lenton, T. M., Daines, S. J. and Mills, B. J. 2018. COPSE reloaded: an improved model of biogeochemical cycling over Phanerozoic time. *Earth-Science Reviews*, **178**, 1–28.

Levin, S. A. 1998. Ecosystems and the biosphere as complex adaptive systems. *Ecosystems*, **1**, 431–436.

Lewis, F., Butler, A. and Gilbert, L. 2011. A unified approach to model selection using the likelihood ratio test. *Methods in Ecology and Evolution*, **2** (2), 155–162.

Lovelock, J. 2016. *Gaia: A new look at life on Earth*. Oxford University Press.

Marković, D. and Gros, C. 2014. Power laws and self-organized criticality in theory and nature. *Physics Reports*, **536** (2), 41–74.

Massey, F. J. Jr 1951. The Kolmogorov-Smirnov test for goodness of fit. *Journal of the American Statistical Association*, **46** (253), 68–78.

McElreath, R. 2018. *Statistical rethinking: A Bayesian course with examples in R and Stan*. Chapman & Hall/CRC.

Middelburg, J. J. 1989. A simple rate model for organic matter decomposition in marine sediments. *Geochimica et Cosmochimica Acta*, **53** (7), 1577–1581.

Mills, B. J., Donnadieu, Y. and Goddéris, Y. 2021. Spatial continuous integration of Phanerozoic global biogeochemistry and climate. *Gondwana Research*, **100**, 73–86.

Morlon, H. 2014. Phylogenetic approaches for studying diversification. *Ecology Letters*, **17** (4), 508–525.

Muscente, A. D., Prabhu, A., Zhong, H., Eleish, A., Meyer, M. B., Fox, P., Hazen, R. M. and Knoll, A. H. 2018. Quantifying ecological impacts of mass extinctions with network analysis of fossil communities. *Proceedings of the National Academy of Sciences*, **115** (20), 5217–5222.

Neath, A. A. and Cavanaugh, J. E. 2012. The Bayesian information criterion: background, derivation, and applications. *Wiley Interdisciplinary Reviews: Computational Statistics*, **4** (2), 199–203.

Newman, M. E. 1996. Self-organized criticality, evolution and the fossil extinction record. *Proceedings of the Royal Society B*, **263** (1376), 1605–1610.

Newman, M. E. 2005. Power laws, Pareto distributions and Zipf's law. *Contemporary Physics*, **46** (5), 323–351.

Newman, M. and Eble, G. J. 1999. Decline in extinction rates and scale invariance in the fossil record. *Paleobiology*, **25** (4), 434–439.

Payne, J. L., Bachan, A., Heim, N. A., Hull, P. M. and Knope, M. L. 2020. The evolution of complex life and the stabilization of the Earth system. *Interface Focus*, **10** (4), 20190106.

Penn, J. L., Deutsch, C., Payne, J. L. and Sperling, E. A. 2018. Temperature-dependent hypoxia explains biogeography and severity of end-Permian marine mass extinction. *Science*, **362** (6419), eaat1327.

Plotnick, R. E. and McKinney, M. L. 1993. Ecosystem organization and extinction dynamics. *Palaios*, **8** (2), 202–212.

Plotnick, R. E. and Sepkoski, J. J. Jr 2001. A multiplicative multifractal model for originations and extinctions. *Paleobiology*, **27** (1), 126–139.

Prigogine, I. 1980. *From being to becoming: Time and complexity in the physical sciences*. Freeman.

Raup, D. M. and Sepkoski, J. J. Jr 1984. Periodicity of extinctions in the geologic past. *Proceedings of the National Academy of Sciences*, **81** (3), 801–805.

Rohde, R. A. and Muller, R. A. 2005. Cycles in fossil diversity. *Nature*, **434** (7030), 208–210.

Rudolf, V. H. W. and Lafferty, K. D. 2011. Stage structure alters how complexity affects stability of ecological networks. *Ecology Letters*, **14** (1), 75–79.

Scheffer, M., Brovkin, V. and Cox, P. M. 2006. Positive feedback between global warming and atmospheric $CO_2$ concentration inferred from past climate change. *Geophysical Research Letters*, **33** (10), L10702.

Schroeder, M. 2009. *Fractals, chaos, power laws: Minutes from an infinite paradise*. Dover Publications.

Schwarz, G. 1978. Estimating the dimension of a model. *The Annals of Statistics*, **6** (2), 461–464.

Scotese, C. R., Song, H., Mills, B. J. and van der Meer, D. G. 2021. Phanerozoic paleotemperatures: the Earth's changing climate during the last 540 million years. *Earth-Science Reviews*, **215**, 103503.

Sepkoski, J. J. Jr 2002. A compendium of fossil marine animal genera. *Bulletins of American Paleontology*, **363**, 1–560.

Shang, H. 2023a. A generic hierarchical model of organic matter degradation and preservation in aquatic systems. *Communications Earth & Environment*, **4** (1), 16.

Shang, H. 2023b. Mineral evolution facilitated Earth's oxidation. *Communications Earth & Environment*, **4** (1), 213.

Shang, H. 2023c. Dichotomous effects of oxidative metabolisms: a theoretical perspective on the dolomite problem. *Global and Planetary Change*, **222**, 104041.

Shang, H. 2024a. Scale-independent variation rates of Phanerozoic environmental variables and implications for Earth's sustainability and habitability. *Mathematical Geosciences*, **56**, 1469–1485.

Shang, H. 2024b. Probing long-lived radioactive isotopes on the double-logarithmic Segrè chart. *Frontiers in Chemistry*, **12**, 1057928.

Shaviv, N. J., Svensmark, H. and Veizer, J. 2023. The Phanerozoic climate. *Annals of the New York Academy of Sciences*, **1519** (1), 7–19.

Sheridan, J. A. and Bickford, D. 2011. Shrinking body size as an ecological response to climate change. *Nature Climate Change*, **1** (8), 401–406.

Simpson, G. G. 1944. *Tempo and mode in evolution*. Columbia University Press.

Simpson, G. G. 1953. *The major features of evolution*. Columbia University Press.

Sneppen, K., Bak, P., Flyvbjerg, H. and Jensen, M. H. 1995. Evolution as a self-organized critical phenomenon. *Proceedings of the National Academy of Sciences*, **92** (11), 5209–5213.

Sole, R. V., Manrubia, S. C., Benton, M. and Bak, P. 1997. Self-similarity of extinction statistics in the fossil record. *Nature*, **388** (6644), 764–767.

Song, H., Kemp, D. B., Tian, L., Chu, D., Song, H. and Dai, X. 2021. Thresholds of temperature change for mass extinctions. *Nature Communications*, **12** (1), 4694.

Sornette, D. and Cont, R. 1997. Convergent multiplicative processes repelled from zero: power laws and truncated power laws. *Journal de Physique I*, **7** (3), 431–444.

Steffen, W., Sanderson, R. A., Tyson, P. D., Jäger, J., Matson, P. A., Moore, B. III, Oldfield, F., Richardson, K., Schellnhuber, H., Turner, B. L. and Wasson, R. J. 2005. *Global change and the Earth system: A planet under pressure*. Springer Science & Business Media.

Sudakov, I., Vakulenko, S. A., Kirievskaya, D. and Golden, K. M. 2017. Large ecosystems in transition: bifurcations and mass extinction. *Ecological Complexity*, **32**, 209–216.

Vérard, C. and Veizer, J. 2019. On plate tectonics and ocean temperatures. *Geology*, **47** (9), 881–885.

Vermeij, G. J. 2006. Historical contingency and the purported uniqueness of evolutionary innovations. *Proceedings of the National Academy of Sciences*, **103** (6), 1804–1809.

Vermeij, G. J. 2024. The illusion of balance in the history of the biosphere. *Geobiology*, **22** (1), e12584.

Vuong, Q. H. 1989. Likelihood ratio tests for model selection and non-nested hypotheses. *Econometrica*, **57** (2), 307–333.

West, G. B. 1999. The origin of universal scaling laws in biology. *Physica A: Statistical Mechanics and its Applications*, **263** (1–4), 104–113.

Yacobucci, M. M. 2005. Multifractal and white noise evolutionary dynamics in Jurassic–Cretaceous Ammonoidea. *Geology*, **33** (2), 97–100.

# Accelerations of the Phanerozoic Biogeosystems – Supporting Information –

Haitao Shang[1,2] *

[1]Department of Earth, Environmental and Resource Sciences

[2]Computational Science Program

The University of Texas at El Paso, El Paso, TX 79968, USA

*To whom correspondence should be addressed; E-mail: htshang.research@gmail.com.

# S1 Information of Datasets

Table S1: Metadata of datasets on genus richness, origination rate, extinction rate, atmospheric $CO_2$ level, and global average temperature. Units of overall time ranges and time steps are million years ago (Ma) and million years (Myr), respectively.

| Quantity | Overall time range | Original time step | Source |
|---|---|---|---|
| Genus richness | 524 Ma – 2 Ma | Stage level | Calculated using the methods in Kocsis et al. (2019) |
| Origination rate | 516 Ma – 2 Ma | Stage level | Calculated using the methods in Kocsis et al. (2019) |
| Extinction rate | 524 Ma – 4 Ma | Stage level | Calculated using the methods in Kocsis et al. (2019) |
| Atmospheric $CO_2$ level | 419 Ma – 0 Ma | 0.5 Myr | Foster et al. (2017) |
| Global average temperature | 540 Ma – 0 Ma | 1 Myr | Scotese et al. (2021) |

# S2 Accelerations in time series interpolated with a 0.05 Myr timestep

Table S2: Best-fitting power law (PL) distributions for negative acceleration (NA), positive acceleration (PA), and all acceleration (AA) of genus richness (GR), origination (OR), extinction (EX), atmospheric $CO_2$ level ($CO_2$), and global average temperature (T). The time step between two consecutive data points in the interpolated time series of these five quantities is 0.05 Myr (Material & Method, Datasets). Reported statistics include the coefficient of determination ($R^2$), root mean square error (RMSE), Kolmogorov-Smirnov test $p$-value ($p_{\mathrm{KS}}$), and Cramér–von Mises test $p$-value ($p_{\mathrm{CM}}$).

| **Quantity** | **Category** | **Best-fitting PL** | $R^2$ | **RMSE** | $p_{\mathrm{KS}}$ | $p_{\mathrm{CM}}$ |
|---|---|---|---|---|---|---|
| Acceleration of genus richness | $\lvert\mathrm{NA_{GR}}\rvert = \{\lvert a_{\mathrm{GR}}\rvert \lvert a_{\mathrm{GR}} < 0\}$ | Count $\sim \lvert\mathrm{NA_{GR}}\rvert^{-2.27}$ | 0.98 | 0.01 | 0.99 | 0.97 |
| | $\lvert\mathrm{PA_{GR}}\rvert = \{a_{\mathrm{GR}} \lvert a_{\mathrm{GR}} > 0\}$ | Count $\sim \lvert\mathrm{PA_{GR}}\rvert^{-2.21}$ | 0.92 | 0.24 | 0.79 | 0.50 |
| | $\lvert\mathrm{AA_{GR}}\rvert = \{\lvert a_{\mathrm{GR}}\rvert \lvert a_{\mathrm{GR}} \neq 0\}$ | Count $\sim \lvert\mathrm{AA_{GR}}\rvert^{-2.59}$ | 0.98 | 0.12 | 0.99 | 0.81 |
| Acceleration of origination | $\lvert\mathrm{NA_{OR}}\rvert = \{\lvert a_{\mathrm{OR}}\rvert \lvert a_{\mathrm{OR}} < 0\}$ | Count $\sim \lvert\mathrm{NA_{OR}}\rvert^{-2.39}$ | 0.97 | 0.15 | 0.79 | 0.54 |
| | $\lvert\mathrm{PA_{OR}}\rvert = \{a_{\mathrm{OR}} \lvert a_{\mathrm{OR}} > 0\}$ | Count $\sim \lvert\mathrm{PA_{OR}}\rvert^{-2.21}$ | 0.94 | 0.22 | 0.78 | 0.68 |
| | $\lvert\mathrm{AA_{OR}}\rvert = \{\lvert a_{\mathrm{OR}}\rvert \lvert a_{\mathrm{OR}} \neq 0\}$ | Count $\sim \lvert\mathrm{AA_{OR}}\rvert^{-2.54}$ | 0.99 | 0.12 | 0.99 | 0.97 |
| Acceleration of extinction | $\lvert\mathrm{NA_{EX}}\rvert = \{\lvert a_{\mathrm{EX}}\rvert \lvert a_{\mathrm{EX}} < 0\}$ | Count $\sim \lvert\mathrm{NA_{EX}}\rvert^{-2.22}$ | 0.93 | 0.24 | 0.79 | 0.63 |
| | $\lvert\mathrm{PA_{EX}}\rvert = \{a_{\mathrm{EX}} \lvert a_{\mathrm{EX}} > 0\}$ | Count $\sim \lvert\mathrm{PA_{EX}}\rvert^{-2.14}$ | 0.94 | 0.20 | 0.99 | 0.86 |
| | $\lvert\mathrm{AA_{EX}}\rvert = \{\lvert a_{\mathrm{EX}}\rvert \lvert a_{\mathrm{EX}} \neq 0\}$ | Count $\sim \lvert\mathrm{AA_{EX}}\rvert^{-2.35}$ | 0.98 | 0.12 | 1.00 | 1.00 |
| Acceleration of $CO_2$ | $\lvert\mathrm{NA_{CO_2}}\rvert = \{\lvert a_{\mathrm{CO_2}}\rvert \lvert a_{\mathrm{CO_2}} < 0\}$ | Count $\sim \lvert\mathrm{NA_{CO_2}}\rvert^{-2.78}$ | 0.98 | 0.13 | 1.00 | 0.99 |
| | $\lvert\mathrm{PA_{CO_2}}\rvert = \{a_{\mathrm{CO_2}} \lvert a_{\mathrm{CO_2}} > 0\}$ | Count $\sim \lvert\mathrm{PA_{CO_2}}\rvert^{-2.81}$ | 0.99 | 0.16 | 0.99 | 0.97 |
| | $\lvert\mathrm{AA_{CO_2}}\rvert = \{\lvert a_{\mathrm{CO_2}}\rvert \lvert a_{\mathrm{CO_2}} \neq 0\}$ | Count $\sim \lvert\mathrm{AA_{CO_2}}\rvert^{-2.82}$ | 0.99 | 0.10 | 1.00 | 0.99 |
| Acceleration of temperature | $\lvert\mathrm{NA_T}\rvert = \{\lvert a_{\mathrm{T}}\rvert \lvert a_{\mathrm{T}} < 0\}$ | Count $\sim \lvert\mathrm{NA_T}\rvert^{-2.64}$ | 0.96 | 0.19 | 0.99 | 0.97 |
| | $\lvert\mathrm{PA_T}\rvert = \{a_{\mathrm{T}} \lvert a_{\mathrm{T}} > 0\}$ | Count $\sim \lvert\mathrm{PA_T}\rvert^{-2.68}$ | 0.92 | 0.31 | 0.79 | 0.63 |
| | $\lvert\mathrm{AA_T}\rvert = \{\lvert a_{\mathrm{T}}\rvert \lvert a_{\mathrm{T}} \neq 0\}$ | Count $\sim \lvert\mathrm{AA_T}\rvert^{-2.74}$ | 0.98 | 0.15 | 0.99 | 0.97 |

Table S3: Best-fitting exponentially truncated power law (ETPL) distributions for negative acceleration (NA), positive acceleration (PA), and all acceleration (AA) of genus richness (GR), origination (OR), extinction (EX), atmospheric $CO_2$ level ($CO_2$), and global average temperature (T). The time step between two consecutive data points in the interpolated time series of these five quantities is 0.05 Myr (Material & Method, Datasets). Reported statistics include the coefficient of determination ($R^2$), root mean square error (RMSE), Kolmogorov-Smirnov test $p$-value ($p_{\mathrm{KS}}$), and Cramér–von Mises test $p$-value ($p_{\mathrm{CM}}$).

| **Quantity** | **Category** | **Best-fitting ETPL** | $\boldsymbol{R^2}$ | **RMSE** | $\boldsymbol{p}_{\mathrm{KS}}$ | $\boldsymbol{p}_{\mathrm{CM}}$ |
|---|---|---|---|---|---|---|
| Acceleration of genus richness | $\lvert\mathrm{NA_{GR}}\rvert = \{\lvert a_{\mathrm{GR}}\rvert \mid a_{\mathrm{GR}} < 0\}$ | Count $\sim \exp\left(-0.02 * \lvert\mathrm{NA_{GR}}\rvert\right) * \lvert\mathrm{NA_{GR}}\rvert^{-1.80}$ | 0.99 | 0.02 | 1.00 | 0.99 |
| | $\lvert\mathrm{PA_{GR}}\rvert = \{a_{\mathrm{GR}} \mid a_{\mathrm{GR}} > 0\}$ | Count $\sim \exp\left(-0.005 * \lvert\mathrm{PA_{GR}}\rvert\right) * \lvert\mathrm{PA_{GR}}\rvert^{-2.20}$ | 0.99 | 0.02 | 0.79 | 0.50 |
| | $\lvert\mathrm{AA_{GR}}\rvert = \{\lvert a_{\mathrm{GR}}\rvert \mid a_{\mathrm{GR}} \neq 0\}$ | Count $\sim \exp\left(-0.009 * \lvert\mathrm{AA_{GR}}\rvert\right) * \lvert\mathrm{AA_{GR}}\rvert^{-2.31}$ | 0.99 | 0.01 | 0.99 | 0.75 |
| Acceleration of origination | $\lvert\mathrm{NA_{OR}}\rvert = \{\lvert a_{\mathrm{OR}}\rvert \mid a_{\mathrm{OR}} < 0\}$ | Count $\sim \exp\left(-3.34 * \lvert\mathrm{NA_{OR}}\rvert\right) * \lvert\mathrm{NA_{OR}}\rvert^{-2.35}$ | 0.99 | 0.002 | 0.79 | 0.54 |
| | $\lvert\mathrm{PA_{OR}}\rvert = \{a_{\mathrm{OR}} \mid a_{\mathrm{OR}} > 0\}$ | Count $\sim \exp\left(-4.82 * \lvert\mathrm{PA_{OR}}\rvert\right) * \lvert\mathrm{PA_{OR}}\rvert^{-2.40}$ | 0.99 | 0.02 | 0.42 | 0.33 |
| | $\lvert\mathrm{AA_{OR}}\rvert = \{\lvert a_{\mathrm{OR}}\rvert \mid a_{\mathrm{OR}} \neq 0\}$ | Count $\sim \exp\left(-3.07 * \lvert\mathrm{AA_{OR}}\rvert\right) * \lvert\mathrm{AA_{OR}}\rvert^{-2.49}$ | 0.99 | 0.004 | 0.99 | 0.92 |
| Acceleration of extinction | $\lvert\mathrm{NA_{EX}}\rvert = \{\lvert a_{\mathrm{EX}}\rvert \mid a_{\mathrm{EX}} < 0\}$ | Count $\sim \exp\left(-3.62 * \lvert\mathrm{NA_{EX}}\rvert\right) * \lvert\mathrm{NA_{EX}}\rvert^{-1.77}$ | 0.97 | 0.05 | 0.42 | 0.20 |
| | $\lvert\mathrm{PA_{EX}}\rvert = \{a_{\mathrm{EX}} \mid a_{\mathrm{EX}} > 0\}$ | Count $\sim \exp\left(-1.59 * \lvert\mathrm{PA_{EX}}\rvert\right) * \lvert\mathrm{PA_{EX}}\rvert^{-2.29}$ | 0.99 | 0.007 | 0.79 | 0.68 |
| | $\lvert\mathrm{AA_{EX}}\rvert = \{\lvert a_{\mathrm{EX}}\rvert \mid a_{\mathrm{EX}} \neq 0\}$ | Count $\sim \exp\left(-0.91 * \lvert\mathrm{AA_{EX}}\rvert\right) * \lvert\mathrm{AA_{EX}}\rvert^{-2.40}$ | 0.99 | 0.02 | 0.009 | 1.00 |
| Acceleration of $CO_2$ | $\lvert\mathrm{NA_{CO_2}}\rvert = \{\lvert a_{\mathrm{CO_2}}\rvert \mid a_{\mathrm{CO_2}} < 0\}$ | Count $\sim \exp\left(-0.0004 * \lvert\mathrm{NA_{CO_2}}\rvert\right) * \lvert\mathrm{NA_{CO_2}}\rvert^{-2.69}$ | 0.99 | 0.01 | 0.79 | 0.68 |
| | $\lvert\mathrm{PA_{CO_2}}\rvert = \{a_{\mathrm{CO_2}} \mid a_{\mathrm{CO_2}} > 0\}$ | Count $\sim \exp\left(-0.0003 * \lvert\mathrm{PA_{CO_2}}\rvert\right) * \lvert\mathrm{PA_{CO_2}}\rvert^{-2.62}$ | 0.99 | 0.001 | 0.99 | 0.92 |
| | $\lvert\mathrm{AA_{CO_2}}\rvert = \{\lvert a_{\mathrm{CO_2}}\rvert \mid a_{\mathrm{CO_2}} \neq 0\}$ | Count $\sim \exp\left(-0.0003 * \lvert\mathrm{AA_{CO_2}}\rvert\right) * \lvert\mathrm{AA_{CO_2}}\rvert^{-2.70}$ | 0.99 | 0.005 | 0.99 | 0.86 |
| Acceleration of temperature | $\lvert\mathrm{NA_T}\rvert = \{\lvert a_{\mathrm{T}}\rvert \mid a_{\mathrm{T}} < 0\}$ | Count $\sim \exp\left(-0.04 * \lvert\mathrm{NA_T}\rvert\right) * \lvert\mathrm{NA_T}\rvert^{-2.13}$ | 0.99 | 0.03 | 0.79 | 0.46 |
| | $\lvert\mathrm{PA_T}\rvert = \{a_{\mathrm{T}} \mid a_{\mathrm{T}} > 0\}$ | Count $\sim \exp\left(-0.02 * \lvert\mathrm{PA_T}\rvert\right) * \lvert\mathrm{PA_T}\rvert^{-2.49}$ | 0.99 | 0.32 | 0.79 | 0.63 |
| | $\lvert\mathrm{AA_T}\rvert = \{\lvert a_{\mathrm{T}}\rvert \mid a_{\mathrm{T}} \neq 0\}$ | Count $\sim \exp\left(-0.04 * \lvert\mathrm{AA_T}\rvert\right) * \lvert\mathrm{AA_T}\rvert^{-2.30}$ | 0.99 | 0.02 | 0.79 | 0.46 |

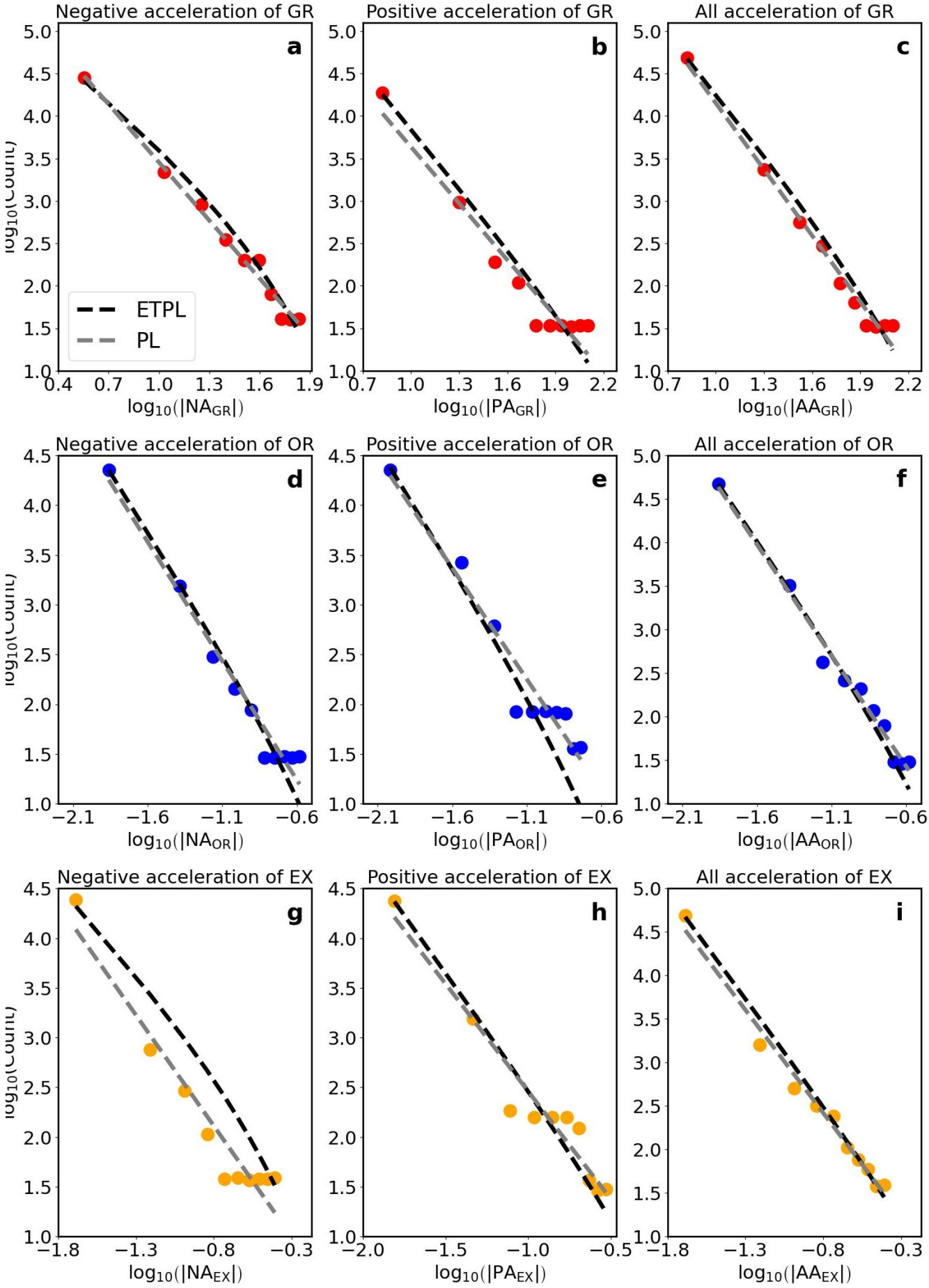
Negative acceleration of GR
Positive acceleration of GR
All acceleration of GR
a
b
c
ETPL
PL
log10(|NAGR|)
log10(|PAGR|)
log10(|AAGR|)
Negative acceleration of OR
Positive acceleration of OR
All acceleration of OR
d
e
f
log10(|NAOR|)
log10(|PAOR|)
log10(|AAOR|)
Negative acceleration of EX
Positive acceleration of EX
All acceleration of EX
g
h
i
log10(|NAEX|)
log10(|PAEX|)
log10(|AAEX|)

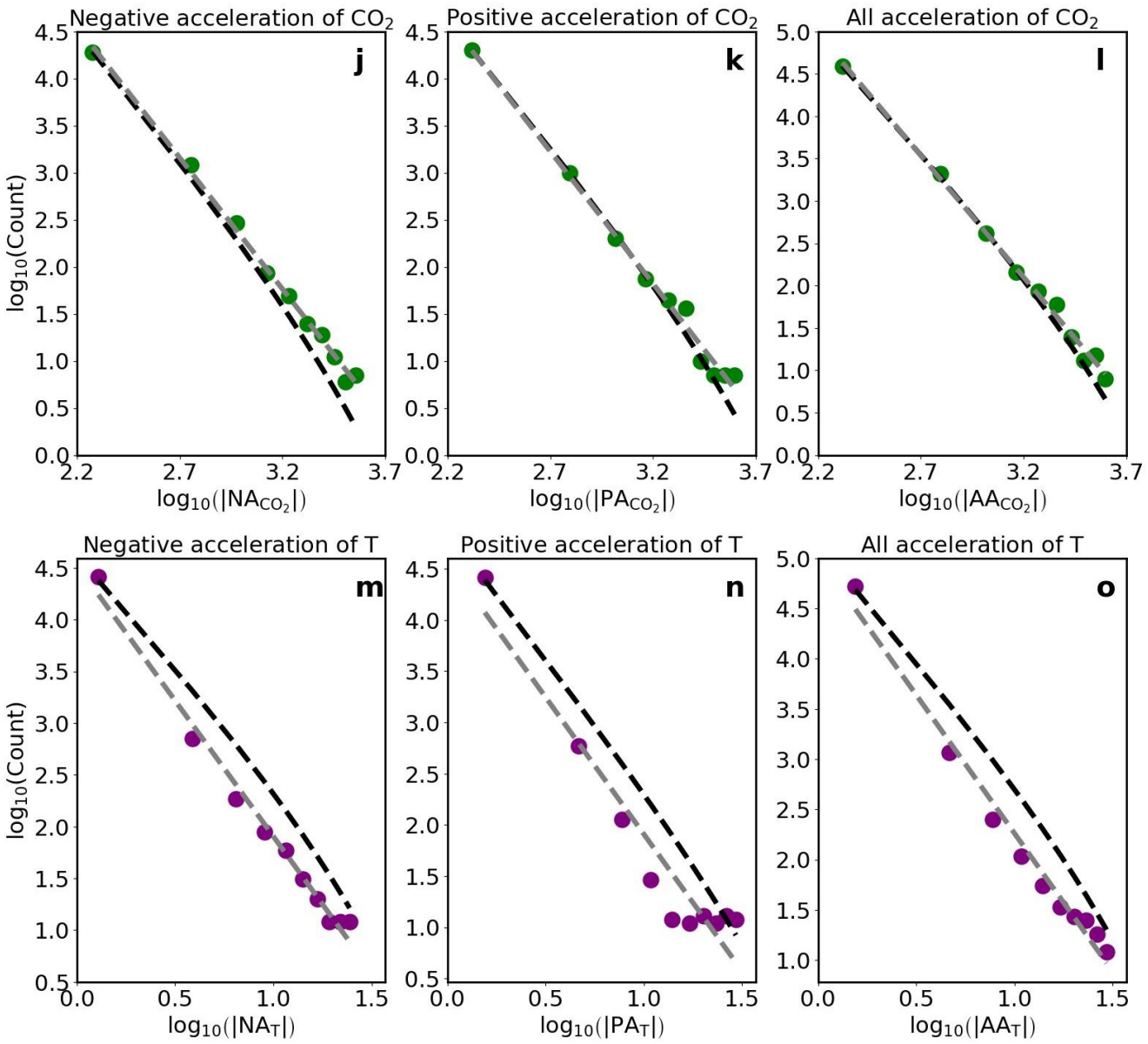


Figure S1: Power law (PL) and exponentially truncated power law (ETPL) distributions of the negative acceleration (NA), positive acceleration (PA), and all acceleration (AA) of (a – c) genus richness (GR), (d – f) origination (OR), (g – i) extinction (EX), (j – l) $CO_2$ level ($CO_2$), and (m – o) global average temperature (T) during the Phanerozoic Eon. The time step between two consecutive data points in the interpolated time series is 0.05 Myr (Material & Method, Datasets). In each panel, the horizontal-axis value for each point is the logarithm of the midpoint of each bin for accelerations, the vertical-axis value for each point is the logarithm of the count in each bin for accelerations, and the black dashed curves and grey dashed lines are the best-fitting ETPL and PL distributions, respectively, for the points at the double logarithmic scale.

# S3 Accelerations of time series interpolated with a 0.01 Myr timestep

Table S4: Best-fitting power law (PL) distributions for negative acceleration (NA), positive acceleration (PA), and all acceleration (AA) of genus richness (GR), origination (OR), extinction (EX), atmospheric $CO_2$ level ($CO_2$), and global average temperature (T). The time step between two consecutive data points in the interpolated time series of these five quantities is 0.01 Myr (Material & Method, Datasets). Reported statistics include the coefficient of determination ($R^2$), root mean square error (RMSE), Kolmogorov-Smirnov test $p$-value ($p_{\mathrm{KS}}$), and Cramér–von Mises test $p$-value ($p_{\mathrm{CM}}$).

| **Quantity** | **Category** | **Best-fitting PL** | $R^2$ | **RMSE** | $p_{\mathrm{KS}}$ | $p_{\mathrm{CM}}$ |
|---|---|---|---|---|---|---|
| Acceleration of genus richness | $\lvert\mathrm{NA_{GR}}\rvert = \{\lvert a_{\mathrm{GR}}\rvert \lvert a_{\mathrm{GR}} < 0\}$ | Count $\sim \lvert\mathrm{NA_{GR}}\rvert^{-2.28}$ | 0.99 | 0.10 | 0.99 | 0.92 |
| | $\lvert\mathrm{PA_{GR}}\rvert = \{a_{\mathrm{GR}} \lvert a_{\mathrm{GR}} > 0\}$ | Count $\sim \lvert\mathrm{PA_{GR}}\rvert^{-2.22}$ | 0.94 | 0.22 | 0.79 | 0.68 |
| | $\lvert\mathrm{AA_{GR}}\rvert = \{\lvert a_{\mathrm{GR}}\rvert \lvert a_{\mathrm{GR}} \neq 0\}$ | Count $\sim \lvert\mathrm{AA_{GR}}\rvert^{-2.60}$ | 0.99 | 0.12 | 0.99 | 0.92 |
| Acceleration of origination | $\lvert\mathrm{NA_{OR}}\rvert = \{\lvert a_{\mathrm{OR}}\rvert \lvert a_{\mathrm{OR}} < 0\}$ | Count $\sim \lvert\mathrm{NA_{OR}}\rvert^{-2.39}$ | 0.97 | 0.15 | 0.79 | 0.68 |
| | $\lvert\mathrm{PA_{OR}}\rvert = \{a_{\mathrm{OR}} \lvert a_{\mathrm{OR}} > 0\}$ | Count $\sim \lvert\mathrm{PA_{OR}}\rvert^{-2.23}$ | 0.94 | 0.21 | 0.79 | 0.68 |
| | $\lvert\mathrm{AA_{OR}}\rvert = \{\lvert a_{\mathrm{OR}}\rvert \lvert a_{\mathrm{OR}} \neq 0\}$ | Count $\sim \lvert\mathrm{AA_{OR}}\rvert^{-2.55}$ | 0.99 | 0.12 | 0.99 | 0.97 |
| Acceleration of extinction | $\lvert\mathrm{NA_{EX}}\rvert = \{\lvert a_{\mathrm{EX}}\rvert \lvert a_{\mathrm{EX}} < 0\}$ | Count $\sim \lvert\mathrm{NA_{EX}}\rvert^{-2.23}$ | 0.93 | 0.23 | 0.79 | 0.54 |
| | $\lvert\mathrm{PA_{EX}}\rvert = \{a_{\mathrm{EX}} \lvert a_{\mathrm{EX}} > 0\}$ | Count $\sim \lvert\mathrm{PA_{EX}}\rvert^{-2.16}$ | 0.94 | 0.20 | 0.99 | 0.86 |
| | $\lvert\mathrm{AA_{EX}}\rvert = \{\lvert a_{\mathrm{EX}}\rvert \lvert a_{\mathrm{EX}} \neq 0\}$ | Count $\sim \lvert\mathrm{AA_{EX}}\rvert^{-2.37}$ | 0.99 | 0.11 | 1.00 | 1.00 |
| Acceleration of $CO_2$ | $\lvert\mathrm{NA_{CO_2}}\rvert = \{\lvert a_{\mathrm{CO_2}}\rvert \lvert a_{\mathrm{CO_2}} < 0\}$ | Count $\sim \lvert\mathrm{NA_{CO_2}}\rvert^{-2.79}$ | 0.99 | 0.07 | 1.00 | 1.00 |
| | $\lvert\mathrm{PA_{CO_2}}\rvert = \{a_{\mathrm{CO_2}} \lvert a_{\mathrm{CO_2}} > 0\}$ | Count $\sim \lvert\mathrm{PA_{CO_2}}\rvert^{-2.81}$ | 0.99 | 0.10 | 0.99 | 0.97 |
| | $\lvert\mathrm{AA_{CO_2}}\rvert = \{\lvert a_{\mathrm{CO_2}}\rvert \lvert a_{\mathrm{CO_2}} \neq 0\}$ | Count $\sim \lvert\mathrm{AA_{CO_2}}\rvert^{-2.88}$ | 1.00 | 0.08 | 1.00 | 1.00 |
| Acceleration of temperature | $\lvert\mathrm{NA_T}\rvert = \{\lvert a_{\mathrm{T}}\rvert \lvert a_{\mathrm{T}} < 0\}$ | Count $\sim \lvert\mathrm{NA_T}\rvert^{-2.62}$ | 0.99 | 0.11 | 0.99 | 0.97 |
| | $\lvert\mathrm{PA_T}\rvert = \{a_{\mathrm{T}} \lvert a_{\mathrm{T}} > 0\}$ | Count $\sim \lvert\mathrm{PA_T}\rvert^{-2.67}$ | 0.93 | 0.29 | 0.79 | 0.68 |
| | $\lvert\mathrm{AA_T}\rvert = \{\lvert a_{\mathrm{T}}\rvert \lvert a_{\mathrm{T}} \neq 0\}$ | Count $\sim \lvert\mathrm{AA_T}\rvert^{-2.75}$ | 0.98 | 0.14 | 0.99 | 0.99 |

Table S5: Best-fitting exponentially truncated power law (ETPL) distributions for negative acceleration (NA), positive acceleration (PA), and all acceleration (AA) of genus richness (GR), origination (OR), extinction (EX), atmospheric $CO_2$ level ($CO_2$), and global average temperature (T). The time step between two consecutive data points in the interpolated time series of these five quantities is 0.01 Myr (Material & Method, Datasets). Reported statistics include the coefficient of determination ($R^2$), root mean square error (RMSE), Kolmogorov-Smirnov test $p$-value ($p_{\mathrm{KS}}$), and Cramér–von Mises test $p$-value ($p_{\mathrm{CM}}$).

| **Quantity** | **Category** | **Best-fitting ETPL** | $R^2$ | **RMSE** | $p_{\mathrm{KS}}$ | $p_{\mathrm{CM}}$ |
|---|---|---|---|---|---|---|
| Acceleration of genus richness | $\lvert\mathrm{NA_{GR}}\rvert = \{\lvert a_{\mathrm{GR}}\rvert \mid a_{\mathrm{GR}} < 0\}$ | Count $\sim \exp\left(-0.03 * \lvert\mathrm{NA_{GR}}\rvert\right) * \lvert\mathrm{NA_{GR}}\rvert^{-1.65}$ | 0.99 | 0.02 | 0.99 | 0.97 |
| | $\lvert\mathrm{PA_{GR}}\rvert = \{a_{\mathrm{GR}} \mid a_{\mathrm{GR}} > 0\}$ | Count $\sim \exp\left(-0.004 * \lvert\mathrm{PA_{GR}}\rvert\right) * \lvert\mathrm{PA_{GR}}\rvert^{-2.29}$ | 0.99 | 0.01 | 0.79 | 0.42 |
| | $\lvert\mathrm{AA_{GR}}\rvert = \{\lvert a_{\mathrm{GR}}\rvert \mid a_{\mathrm{GR}} \neq 0\}$ | Count $\sim \exp\left(-0.009 * \lvert\mathrm{AA_{GR}}\rvert\right) * \lvert\mathrm{AA_{GR}}\rvert^{-2.30}$ | 0.99 | 0.01 | 0.99 | 0.92 |
| Acceleration of origination | $\lvert\mathrm{NA_{OR}}\rvert = \{\lvert a_{\mathrm{OR}}\rvert \mid a_{\mathrm{OR}} < 0\}$ | Count $\sim \exp\left(-3.49 * \lvert\mathrm{NA_{OR}}\rvert\right) * \lvert\mathrm{NA_{OR}}\rvert^{-2.34}$ | 0.99 | 0.003 | 0.79 | 0.86 |
| | $\lvert\mathrm{PA_{OR}}\rvert = \{a_{\mathrm{OR}} \mid a_{\mathrm{OR}} > 0\}$ | Count $\sim \exp\left(-5.06 * \lvert\mathrm{PA_{OR}}\rvert\right) * \lvert\mathrm{PA_{OR}}\rvert^{-2.38}$ | 0.99 | 0.02 | 0.42 | 0.36 |
| | $\lvert\mathrm{AA_{OR}}\rvert = \{\lvert a_{\mathrm{OR}}\rvert \mid a_{\mathrm{OR}} \neq 0\}$ | Count $\sim \exp\left(-3.19 * \lvert\mathrm{AA_{OR}}\rvert\right) * \lvert\mathrm{AA_{OR}}\rvert^{-2.48}$ | 0.99 | 0.003 | 0.99 | 0.97 |
| Acceleration of extinction | $\lvert\mathrm{NA_{EX}}\rvert = \{\lvert a_{\mathrm{EX}}\rvert \mid a_{\mathrm{EX}} < 0\}$ | Count $\sim \exp\left(-3.78 * \lvert\mathrm{NA_{EX}}\rvert\right) * \lvert\mathrm{NA_{EX}}\rvert^{-1.72}$ | 0.97 | 0.05 | 0.17 | 0.15 |
| | $\lvert\mathrm{PA_{EX}}\rvert = \{a_{\mathrm{EX}} \mid a_{\mathrm{EX}} > 0\}$ | Count $\sim \exp\left(-1.63 * \lvert\mathrm{PA_{EX}}\rvert\right) * \lvert\mathrm{PA_{EX}}\rvert^{-2.29}$ | 0.99 | 0.008 | 0.99 | 0.81 |
| | $\lvert\mathrm{AA_{EX}}\rvert = \{\lvert a_{\mathrm{EX}}\rvert \mid a_{\mathrm{EX}} \neq 0\}$ | Count $\sim \exp\left(-0.91 * \lvert\mathrm{AA_{EX}}\rvert\right) * \lvert\mathrm{AA_{EX}}\rvert^{-2.40}$ | 0.99 | 0.02 | 1.00 | 1.00 |
| Acceleration of $CO_2$ | $\lvert\mathrm{NA_{CO_2}}\rvert = \{\lvert a_{\mathrm{CO_2}}\rvert \mid a_{\mathrm{CO_2}} < 0\}$ | Count $\sim \exp\left(-0.0004 * \lvert\mathrm{NA_{CO_2}}\rvert\right) * \lvert\mathrm{NA_{CO_2}}\rvert^{-2.68}$ | 0.99 | 0.009 | 0.79 | 0.75 |
| | $\lvert\mathrm{PA_{CO_2}}\rvert = \{a_{\mathrm{CO_2}} \mid a_{\mathrm{CO_2}} > 0\}$ | Count $\sim \exp\left(-0.0003 * \lvert\mathrm{PA_{CO_2}}\rvert\right) * \lvert\mathrm{PA_{CO_2}}\rvert^{-2.63}$ | 0.99 | 0.0005 | 0.79 | 0.81 |
| | $\lvert\mathrm{AA_{CO_2}}\rvert = \{\lvert a_{\mathrm{CO_2}}\rvert \mid a_{\mathrm{CO_2}} \neq 0\}$ | Count $\sim \exp\left(-0.0004 * \lvert\mathrm{AA_{CO_2}}\rvert\right) * \lvert\mathrm{AA_{CO_2}}\rvert^{-2.63}$ | 0.99 | 0.002 | 0.99 | 0.97 |
| Acceleration of temperature | $\lvert\mathrm{NA_T}\rvert = \{\lvert a_{\mathrm{T}}\rvert \mid a_{\mathrm{T}} < 0\}$ | Count $\sim \exp\left(-0.04 * \lvert\mathrm{NA_T}\rvert\right) * \lvert\mathrm{NA_T}\rvert^{-2.12}$ | 0.99 | 0.03 | 0.79 | 0.39 |
| | $\lvert\mathrm{PA_T}\rvert = \{a_{\mathrm{T}} \mid a_{\mathrm{T}} > 0\}$ | Count $\sim \exp\left(-0.03 * \lvert\mathrm{PA_T}\rvert\right) * \lvert\mathrm{PA_T}\rvert^{-2.47}$ | 0.99 | 0.02 | 0.42 | 0.36 |
| | $\lvert\mathrm{AA_T}\rvert = \{\lvert a_{\mathrm{T}}\rvert \mid a_{\mathrm{T}} \neq 0\}$ | Count $\sim \exp\left(-0.04 * \lvert\mathrm{AA_T}\rvert\right) * \lvert\mathrm{AA_T}\rvert^{-2.28}$ | 0.99 | 0.01 | 0.99 | 0.94 |

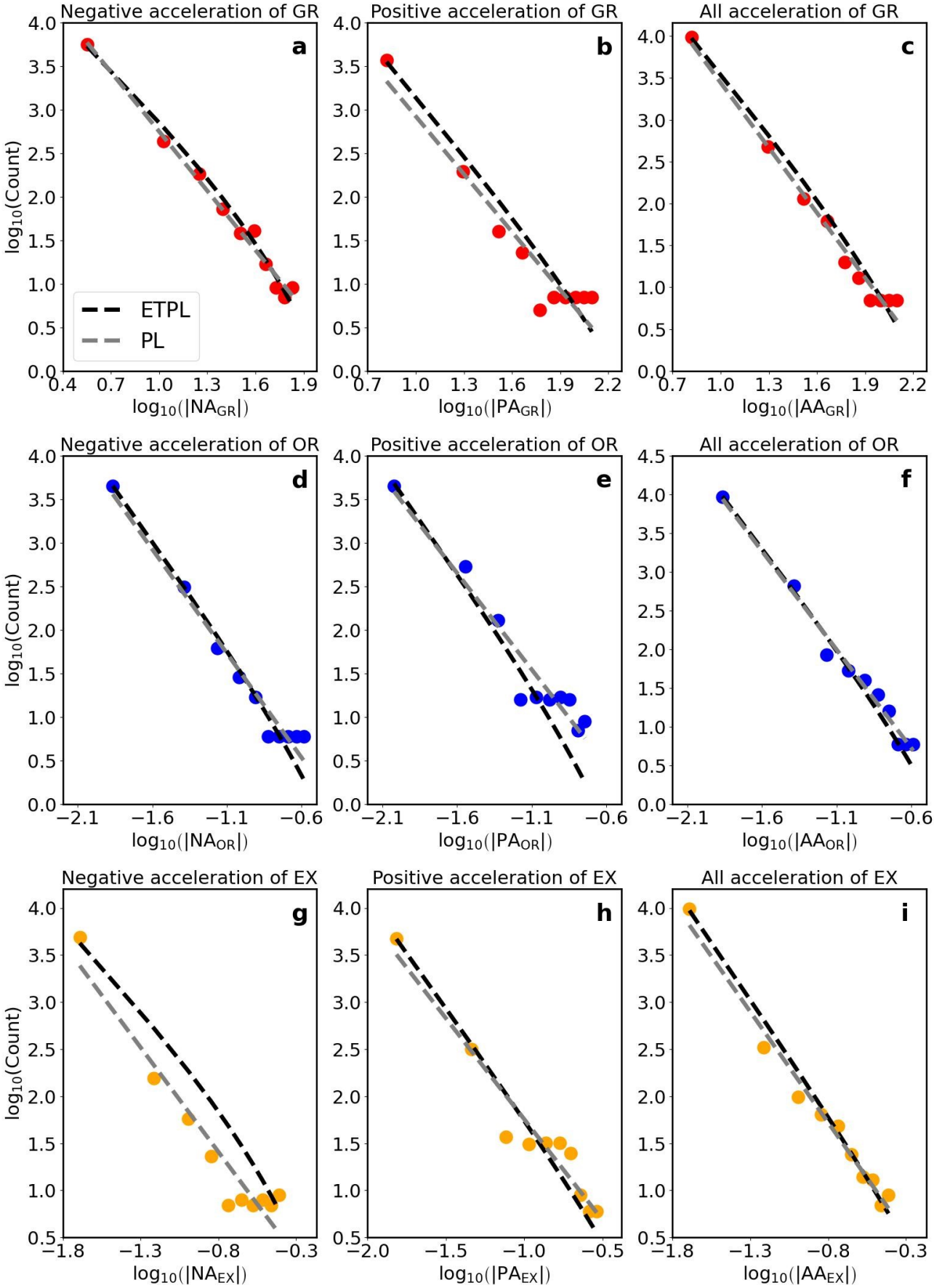
Negative acceleration of GR
a
Positive acceleration of GR
b
All acceleration of GR
c
Negative acceleration of OR
d
Positive acceleration of OR
e
All acceleration of OR
f
Negative acceleration of EX
g
Positive acceleration of EX
h
All acceleration of EX
i
ETPL
PL
log10(Count)
log10(|NAGR|)
log10(|PAGR|)
log10(|AAGR|)
log10(|NAOR|)
log10(|PAOR|)
log10(|AAOR|)
log10(|NAEX|)
log10(|PAEX|)
log10(|AAEX|)

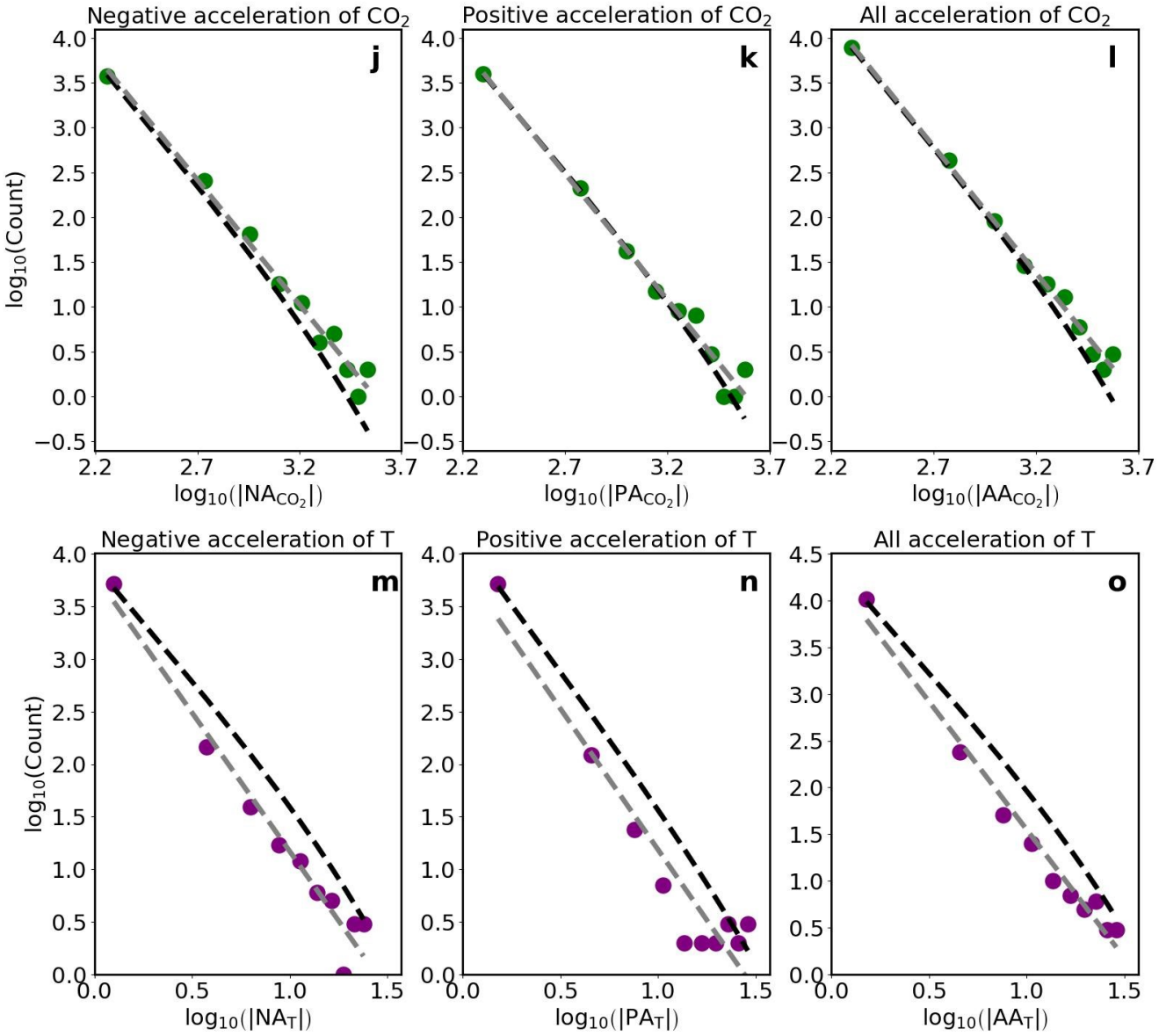


Figure S2: Power law (PL) and exponentially truncated power law (ETPL) distributions of the negative acceleration (NA), positive acceleration (PA), and all acceleration (AA) of (a – c) genus richness (GR), (d – f) origination (OR), (g – i) extinction (EX), (j – l) atmospheric $CO_2$ level ($CO_2$), and (m – o) global average temperature (T) during the Phanerozoic Eon. The time step between two consecutive data points in the interpolated time series is 0.01 Myr (Material & Method, Datasets). In each panel, the horizontal-axis value for each point is the logarithm of the midpoint of each bin for accelerations, the vertical-axis value for each point is the logarithm of the count in each bin for accelerations, and the black dashed curves and grey dashed lines are the best-fitting ETPL and PL distributions, respectively, for the points at the double logarithmic scale.

# S4 Pearson correlation analyses

Table S6: Summary of the Pearson correlation coefficient values (Pearson's $r$) and $p$-values ($p_r$) for the accelerations of each pair of variables ($a_{\text{GR}}$, $a_{\text{OR}}$, $a_{\text{EX}}$, $a_{\text{CO}_2}$, and $a_{\text{T}}$) and the absolute values of these accelerations ($|a_{\text{GR}}|$, $|a_{\text{OR}}|$, $|a_{\text{EX}}|$, $|a_{\text{CO}_2}|$, and $|a_{\text{T}}|$). These Pearson's $r$ values are visualized in Figure S3. The Spearman's rank correlation coefficient values (Spearman's $\rho$) and $p$-values ($p_\rho$) for these accelerations are presented in Table 10 and Figure 3. Note that the analysis and discussion about the temporal correlations among these accelerations are primarily based on Spearman's $\rho$ values because these accelerations are neither the standard normal distribution nor approximately normally distributed (Material & Method, Correlation Analysis).

| **Quantity** | **Variable pair** | **Pearson's $r$** | $p_r$ |
|---|---|---|---|
| Accelerations of biological metrics & environmental variables | $a_{\text{GR}}$ vs. $a_{\text{OR}}$ | $\mathbf{-0.62}$ | $\mathbf{\ll 0.05}$ |
| | $a_{\text{GR}}$ vs. $a_{\text{EX}}$ | $\mathbf{0.73}$ | $\mathbf{\ll 0.05}$ |
| | $a_{\text{GR}}$ vs. $a_{\text{CO}_2}$ | $-0.01$ | $0.89$ |
| | $a_{\text{GR}}$ vs. $a_{\text{T}}$ | $\mathbf{-0.14}$ | $\mathbf{\ll 0.05}$ |
| | $a_{\text{OR}}$ vs. $a_{\text{EX}}$ | $\mathbf{-0.63}$ | $\mathbf{\ll 0.05}$ |
| | $a_{\text{OR}}$ vs. $a_{\text{CO}_2}$ | $0.01$ | $0.85$ |
| | $a_{\text{OR}}$ vs. $a_{\text{T}}$ | $\mathbf{0.11}$ | $\mathbf{0.03}$ |
| | $a_{\text{EX}}$ vs. $a_{\text{CO}_2}$ | $-0.01$ | $0.85$ |
| | $a_{\text{EX}}$ vs. $a_{\text{T}}$ | $\mathbf{-0.13}$ | $\mathbf{\ll 0.05}$ |
| | $a_{\text{CO}_2}$ vs. $a_{\text{T}}$ | $0.04$ | $0.37$ |
| Absolute values of the accelerations of biological metrics & environmental variables | $\lvert a_{\text{GR}}\rvert$ vs. $\lvert a_{\text{OR}}\rvert$ | $\mathbf{0.79}$ | $\mathbf{\ll 0.05}$ |
| | $\lvert a_{\text{GR}}\rvert$ vs. $\lvert a_{\text{EX}}\rvert$ | $\mathbf{0.76}$ | $\mathbf{\ll 0.05}$ |
| | $\lvert a_{\text{GR}}\rvert$ vs. $\lvert a_{\text{CO}_2}\rvert$ | $-0.04$ | $0.36$ |
| | $\lvert a_{\text{GR}}\rvert$ vs. $\lvert a_{\text{T}}\rvert$ | $\mathbf{0.29}$ | $\mathbf{\ll 0.05}$ |
| | $\lvert a_{\text{OR}}\rvert$ vs. $\lvert a_{\text{EX}}\rvert$ | $\mathbf{0.71}$ | $\mathbf{\ll 0.05}$ |
| | $\lvert a_{\text{OR}}\rvert$ vs. $\lvert a_{\text{CO}_2}\rvert$ | $-0.04$ | $0.67$ |
| | $\lvert a_{\text{OR}}\rvert$ vs. $\lvert a_{\text{T}}\rvert$ | $\mathbf{0.20}$ | $\mathbf{\ll 0.05}$ |
| | $\lvert a_{\text{EX}}\rvert$ vs. $\lvert a_{\text{CO}_2}\rvert$ | $-0.05$ | $0.33$ |
| | $\lvert a_{\text{EX}}\rvert$ vs. $\lvert a_{\text{T}}\rvert$ | $\mathbf{0.24}$ | $\mathbf{\ll 0.05}$ |
| | $\lvert a_{\text{CO}_2}\rvert$ vs. $\lvert a_{\text{T}}\rvert$ | $-0.01$ | $0.79$ |

Table S7: Summary of Pearson correlation coefficient values (Pearson's $r$) and $p$-values ($p_r$) for (1) biological metrics' accelerations ($a_{\text{GR}}$, $a_{\text{OR}}$, $a_{\text{EX}}$) versus environmental variables ($\text{CO}_2$ and $\text{T}$), and (2) biological metrics' accelerations ($a_{\text{GR}}$, $a_{\text{OR}}$, $a_{\text{EX}}$) versus environmental variables' variation rates ($R_{\text{CO}_2}$ and $R_{\text{T}}$). The purpose of investigating the correlations among these quantities is to explore whether environmental changes may exert selection pressures on organisms and influence the accelerations of the biological metrics. The Spearman's rank correlation coefficient values (Spearman's $\rho$) and $p$-values ($p_\rho$) for these accelerations are presented in Table 11. Note that the analysis and discussion about the temporal correlations among these quantities are primarily based on Spearman's $\rho$ values because these variables and their variation rates and accelerations are neither the standard normal distribution nor approximately normally distributed (Material $\&$ Method, Correlation Analysis).

| **Quantity** | **Variable pair** | **Pearson's $r$** | $p_r$ |
|---|---|---|---|
| Biological metrics' accelerations *versus* environmental variables | $a_{\text{GR}}$ vs. $\text{CO}_2$ | $-0.02$ | 0.71 |
| | $a_{\text{GR}}$ vs. T | $\mathbf{0.14}$ | $\mathbf{0.01}$ |
| | $a_{\text{OR}}$ vs. $\text{CO}_2$ | $-0.01$ | 0.90 |
| | $a_{\text{OR}}$ vs. T | $-0.05$ | 0.28 |
| | $a_{\text{EX}}$ vs. $\text{CO}_2$ | $-0.004$ | 0.93 |
| | $a_{\text{EX}}$ vs. T | 0.06 | 0.26 |
| Biological metrics' accelerations *versus* environmental variables' variation rates | $a_{\text{GR}}$ vs. $R_{\text{CO}_2}$ | $-0.02$ | 0.65 |
| | $a_{\text{GR}}$ vs. $R_{\text{T}}$ | $-0.02$ | 0.62 |
| | $a_{\text{OR}}$ vs. $R_{\text{CO}_2}$ | 0.05 | 0.28 |
| | $a_{\text{OR}}$ vs. $R_{\text{T}}$ | $\mathbf{0.13}$ | $\mathbf{0.01}$ |
| | $a_{\text{EX}}$ vs. $R_{\text{CO}_2}$ | $-0.03$ | 0.59 |
| | $a_{\text{EX}}$ vs. $R_{\text{T}}$ | $\mathbf{0.16}$ | $\ll \mathbf{0.05}$ |

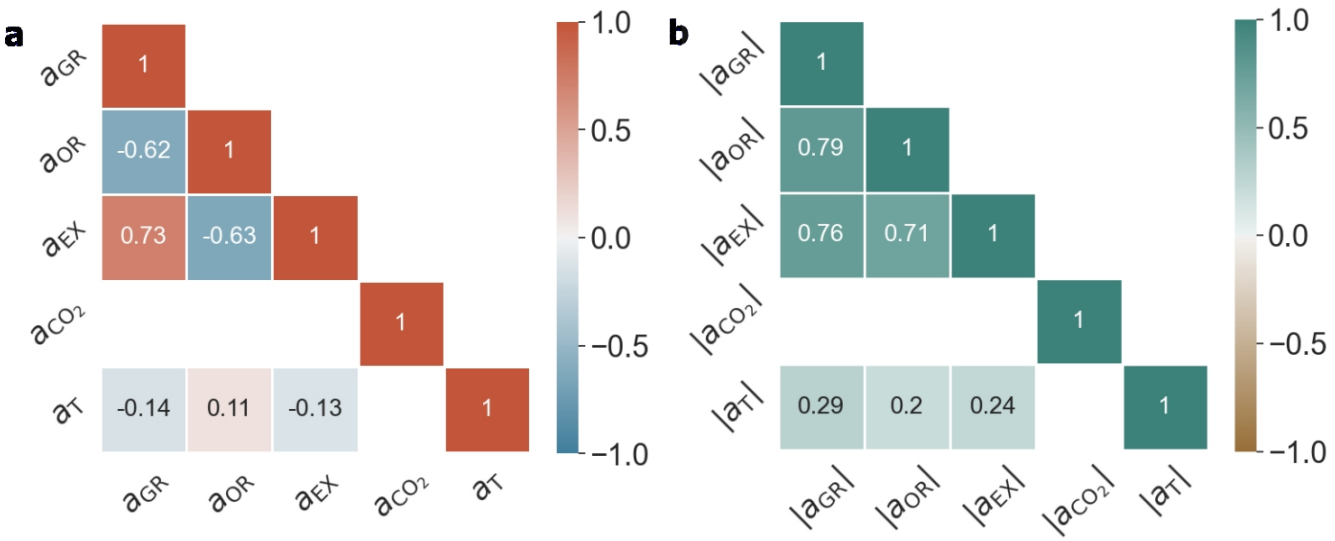


Figure S3: (a) Heatmap of the Pearson correlation coefficient values (Pearson's $r$) for the accelerations ($a$) of genus richness (GR), origination (OR), extinction (EX), atmospheric $CO_2$ level ($CO_2$), and global average temperature (T). The accelerations of these five quantities are denoted as $a_{GR}$, $a_{OR}$, $a_{EX}$, $a_{CO_2}$, and $a_T$, respectively. (b) Heatmap of the Pearson's $r$ values for the absolute values of the accelerations of these five quantities ($|a_{GR}|$, $|a_{OR}|$, $|a_{EX}|$, $|a_{CO_2}|$, and $|a_T|$). A blank cell in the lower triangle in panel (a) or (b) indicates that the $p$-value of the Pearson's $r$ for that pair of accelerations represented by this cell is greater than 0.05 and therefore this Pearson's $r$ value is not statistically significant.

# References

Foster, G. L., D. L. Royer, and D. J. Lunt (2017). Future climate forcing potentially without precedent in the last 420 million years. *Nature Communications 8*, 14845.

Kocsis, Á. T., C. J. Reddin, J. Alroy, and W. Kiessling (2019). The R package divDyn for quantifying diversity dynamics using fossil sampling data. *Methods in Ecology and Evolution 10*(5), 735–743.

Scotese, C. R., H. Song, B. J. Mills, and D. G. van der Meer (2021). Phanerozoic paleotemperatures: The Earth's changing climate during the last 540 million years. *Earth-Science Reviews 215*, 103503.